40AR/39AR CHRONOLOGY OF VOLCANIC EVENTS IN THE AND-1B
DRILLCORE – IMPLICATIONS FOR AGE MODELS AND GLACIAL HISTORY
OF THE ROSS EMBAYMENT

by

Jake I. Ross
William C. McIntosh
Nelia W. Dunbar

NEW MEXICO INSTITUTE OF MINING AND TECHNOLOGY
GEOCHEMISTRY PROGRAM
SOCORRO, NEW MEXICO

AUGUST, 2009

This report was also submitted by Jake I. Ross as an Independent Study in
partial fulfillment of the requirements of the M.S. Degree in Geochemistry

^{40}Ar/^{39}Ar chronology of volcanic events in the AND-1B drillcore – implications for age models and glacial history of the Ross Embayment.

Ross, J. I. (jirhiker@nmt.edu)^{a*}, McIntosh, W. C. (mcintosh@nmt.edu)^{a,b}, and Dunbar, N. W. (nelia@nmt.edu) ^{b}

^{a} Department of Earth and Environmental Science, New Mexico Tech, 801 Leroy Place, Socorro, New Mexico 87801, USA
^{b} New Mexico Bureau of Geology and Mineral Resources, 801 Leroy Place, Socorro, New Mexico 87801, USA
* corresponding author Tel: +1 575 835 5994

Abstract
        ^{40}Ar/^{39}Ar dating of a suite of volcanic clasts and tephra, collected throughout the AND-1B drill core, significantly aids the development of an age-depth model. High precision dates determined for a variety of volcanic materials provide pinning points for constraining the chronostratigraphy of the drill core. The volcanic materials we have dated include 1) felsic and basaltic tephra, 2) interior of an ~3 m thick intermediate lava flow and 3) felsic and basaltic volcanic clasts. Two felsic tephra, two basaltic tephra and the intermediate lava flow yield precise and accurate depositional ages, whereas the volcanic clasts provide maximum depositional ages. The ages for eight stratigraphic intervals are 1) 17.17-17.18 mbsf, basaltic clast (maximum depositional age 0.310±0.039 Ma, all errors quoted at 2σ), 2) 52.80-52.82 mbsf, three basaltic clasts (maximum depositional age 0.726±0.052 Ma), 3) 85.27-85.87 mbsf felsic tephra (1.014±0.008 Ma), 4) ~112-145 mbsf sequence of basaltic tephra (1.633±0.057 to 1.683±0.055 Ma), 5) 480.97-481.96 mbsf pumice-rich mudstone (4.800±0.076 Ma), 6) 646.30-649.34 mbsf intermediate lava flow (6.48±0.13 Ma), 7) 822.78 mbsf kaersutite phenocrysts from volcanic clasts (maximum depositional age 8.53±0.53 Ma) and 8) ~1280 mbsf, three volcanic clasts (maximum depositional age 13.57±0.13 Ma).

        Incremental heating analyses of glass shards from the basaltic tephra display a reproducible saddle-shaped spectrum with discordant apparent ages. Two out of more than twenty-five basaltic glass analyses yield both a statistically defined plateau and precise inverse isochron age. The remainder of the analyses yield discordant apparent ages for all steps and statistically unconstrained isochron ages. Recoil effects, excess ^{40}Ar, and xenocrystic contamination are possible explanations for the observed discordance.

        Volcanic clasts provide the best means of constraining the age of the drill core at depths >600 mbsf. Electron microprobe characterization of numerous volcanic intervals below ~600 mbsf indicates high degrees of alteration in the felsic and basaltic tephra, whereas the volcanic clasts show little to no alteration. The paucity of fresh tephra at depths greater than ~600 mbsf requires age constraints for this interval of the drill core to rely on dating populations of volcanic clasts. Although volcanic clasts do not provide accurate time-

stratigraphic pinning points they do yield accurate maximum depositional ages and are important for provenance studies.

Keywords

1. Introduction

The AND-1B drill core was recovered near Hut Point Peninsula, Ross Island, Antarctica, as part of an international effort to sample a near continuous sedimentary record in southern McMurdo Sound (ANDRILL MIS Project), with the goal of reconstructing the Cenozoic paleoenvironment and paleoclimate of Antarctica. The ANDRILL MIS project drilled into the baythmetric and depocentral axis of a flexural moat formed by the Quaternary volcanic loading of the crust by Ross Island (Horgan et al. 2005). The recovered drill core, AND-1B, reached a depth of 1284.87 meters below sea floor (mbsf), sampling >1200 m of alternating glacial and interglacial sediments interbedded with volcanic and volcaniclastic layers. (Naish et al., 2007).

Meaningful interpretation of the paleoenvironmental record sampled by the AND-1B drill core requires an accurate chronology. This paper reports results of ^{40}Ar/^{39}Ar dating of volcanic materials sampled from eight stratigraphic intervals in the AND-1B drill core, including felsic pumices, basaltic tephra and scattered volcanic clasts.

Volcanic material is located throughout the drill core. However, only a few select intervals have been demonstrated to provide accurate time stratigraphic

pinning points. Four types of material have been dated: felsic tephra, basaltic tephra, an intermediate lava flow, and basaltic and intermediate clasts. The tephra and lava flow yield accurate depositional ages, if 1) they were deposited shortly (<10's of ka) after eruption and 2) yield accurate $^{40}Ar/^{39}Ar$ ages. Volcanic clasts, however, because of the significant time between eruption and deposition, only yield a maximum depositional age.

AND-1B contains a paucity of unaltered felsic tephra suitable for $^{40}Ar/^{39}Ar$ dating. Feldspar phenocrysts, however, from the two fresh felsic tephra reported in this paper, yield the highest precision and most accurate depositional ages. Fresh felsic tephra provide the best targets for $^{40}Ar/^{39}Ar$ dating because they commonly contain potassium-rich feldspar phenocrysts that accurately and precisely record the time of eruption (McIntosh 2001). The highest precision age of all analyses was obtained from euhedral K-feldspar phenocrysts separated from a pure phonolitic-trachytic/traydacitic tephra layer at 85.27-85.87 mbsf. A mudstone layer located from ~481.00-482.00 mbsf contains numerous but dispersed felsic pumice clasts. Although this interval is not a concentrated primary tephra we believe it nonetheless provides a precise and accurate time-stratigraphic horizon because 1) it is compromised of a zone of numerous pumice clasts and, 2) the preservation of delicate pumices suggests limited transportation.

Basaltic tephra layers are abundant within the upper 150 mbsf of the drill core. A sequence of basaltic tephra inter-bedded with glacimarine sediments between ~110-150 mbsf is an important target for dating and volcanic study.

Pompilio et al., (2007) inferred that these layers are derived primarily from subaerial Hawaiian/Strombolian eruptions from vents on Hut Point Peninsula. Back Scatter Electron (BSE) images of the tephra indicate they are composed of abundant angular glass shards with minor amounts of plagioclase and/or olivine/pyroxene micro-phenocrysts. The preservation of the fragile angular glass shards and lack of rounding (Fig. 1C and D), suggests these tephra have not experienced significant mass flow processes and were deposited by settling through the water column shortly after eruption (P. Kyle personal communication, Feb. 2009). The lack of K-rich phenocrysts, such as sanidine, anorthoclase or kaersutite within the basaltic tephra requires analysis of the basaltic glass shards to determine an accurate eruption age. Quantitative microprobe analysis of glass shards yields K_2O values ranging from ~1 to 3% (Appendix B. Table 1.)

An approximately 3 m thick subaqueous lava flow at 636.49-649.30 mbsf provides an additional accurate $^{40}Ar/^{39}Ar$ age used to form the age-depth model. This intermediate lava flow is located in the largest volcanic succession within the core and separates two thick volcaniclastic intervals. The upper and lower contacts of the flow display a thin glassy margin, subsequently replaced by clay minerals. (Pompilio et al., 2007).

Volcanic clasts are abundant within the AND-1B drill core (Talarico et al., 2007), and provide good potential targets for $^{40}Ar/^{39}Ar$ dating. Fifteen basaltic to intermediate clasts ranging from 10 to 25 mm in diameter have been sampled and dated. Although these clasts do not provide accurate depositional ages for the intervals in which they are found, the clasts nevertheless yield accurate

maximum depositional ages, which are useful in constraining the chronology of the drill core. Age data for volcanic clasts are useful for provenance studies, which can provide important insights into past ice flow paths (Talarico et al., 2007; Sandroni et al., 2006).

2. Methods

2.1. Sample Preparation

Samples were prepared at the New Mexico Geochronology Research Laboratory (NMGRL) in Socorro, New Mexico, with the exception of the sample 85-01, which was prepared at McMurdo Station, Ross Island Antarctica. Sample preparation was tailored to each sample in order to optimize results. In general, the sample preparation process consisted of the following steps: mechanical crushing and hand sieving followed by extensive ultrasonic washing and acid treatment. Hand picking, the final sample preparation step, is used to remove any remaining contaminants from the separate. See Table 1 for additional sample preparation information.

2.2. Irradiation

Samples were packaged with flux monitors of known age (Fish Canyon Tuff sanidine, 28.02 Ma; Renne et al., 1998), and irradiated at the reactor facility at Texas A & M, College Park, TX. See table 1. for more information on irradiation procedures.

2.3. Analysis

$^{40}Ar/^{39}Ar$ analyses were performed at NMGRL. Gas extraction was

conducted in a fully automated all-metal extraction system, using either the 50W CO_2 laser or double vacuum Mo resistance furnace systems. Isotopic ratios were determined using a MAP215-50 mass spectrometer by peak jumping in static mode. Further information on the instrumentation used at NMGRL, as well as details for analytical procedures, are located in the notes section of Table 1 and in McIntosh and Chamberlain (1994).

3. Results

Multiple analyses of eight volcanic intervals provide accurate and precise eruption ages. The volcanic samples separated from these eight intervals can be placed into 4 categories: 1) felsic tephra, 2) basaltic tephra, 3) intermediate lava, and 4) volcanic clasts. The precision and accuracy of the $^{40}Ar/^{39}Ar$ ages used to constrain depositional ages for the volcanic intervals are highly dependent on the sample material. The tephra and in-place intermediate lava flow provide accurate depositional ages of variable precision (0.8 – 2.0 %), whereas the volcanic clasts, because of the unknown time between eruption and deposition, yield precise maximum depositional ages. A summary of the $^{40}Ar/^{39}Ar$ ages used to constrain the AND-1B age-model (G. Wilson this volume) is given by Table 1. Tabulated $^{40}Ar/^{39}Ar$ results are listed in Appendix A.

3.1. 17.17-01 (17.17-17.18 mbsf)

A furnace incremental heating analysis of a groundmass concentrate from a volcanic clast sampled at 17.17-17.18 mbsf yields a statistically robust plateau age of 0.310±0.039 Ma (MSWD=1.48, Fig. 2A). The radiogenic yield (% $^{40}Ar^*$) of

this analysis is low but consistent, ranging from 2-6% for 99.5 % of the gas released, followed by an anomalously high radiogenic yield at the last step, which is most likely caused by degassing of the furnace at high temperature. K/Ca values range from 0.17 to 3.2, with an anomalously high value of 16.8 for the first step. The K/Ca values display a systematic decrease with increasing temperature, indicative of the initial degassing and dominance of the system by K-bearing plagioclase phenocrysts and matrix glass, followed by an exhaustion of argon from these reservoirs and a system dominated by the degassing of Ca-rich and K-poor phenocrysts, such as clinopyroxene and olivine (Olmsted 2000).

A plot of the plateau steps on an inverse isochron diagram (Fig. 3A) as described in (Dalrymple et al., 1988) indicates a trapped argon component ($^{40}Ar/^{36}Ar_{intercept}$ = 299.0±2.6) that is statistically indistinguishable from that of the atmosphere ($^{40}Ar/^{36}Ar_{atm}$ = 295.5 Nier, 1950). Compared to the plateau age, the inverse isochron yields a younger, but less precise age of 0.22±0.07 (MSWD=0.33). The two dates, however, overlap at 2σ , and in conjunction with the near atmospheric $^{40}Ar/^{36}Ar$-intercept we infer that excess ^{40}Ar is not a contributing factor to the age of this analysis. The maximum depositional age for sediment at 17.17-17.18 mbsf therefore is given by the 17.17-01 plateau age, 0.310±0.039 Ma.

3.2. 52.80A-01, 52.80B-01, 52.80C-01 (52.80-52.82 mbsf)

Incremental heating in the furnace of a groundmass concentrate (52.80A-01) from a volcanic clast sampled at 52.80-52.82 mbsf yields a statistically robust and precise plateau age of 0.726±0.052 Ma (MSWD=1.35, Fig. 2B). The plateau

represents 100% of the gas released, adding confidence in the apparent age. An inverse isochron plot (Fig. 3B) yields a $^{40}Ar/^{36}Ar$ intercept (294.5±2.2) statistically equivalent to the atmospheric value, indicating that excess ^{40}Ar is not a significant factor in the age of this sample. Radiogenic yields are low, with a maximum value of 10.6%. K/Ca ratios show a trend typical of basaltic groundmass analyses, i.e. decreasing K/Ca with increasing temperature.

Analysis of two other volcanic clasts sampled from the same interval, 52.80-52.82 mbsf, yield statistically older plateau ages (52.80B-01 7.25±0.39, MSWD=2.29; 52.80C-01 0.908±0.059 Ma, MSWD = 1.94, Fig. 2C and D) than that of 52.80A-01. The maximum depositional age for the 52.80-52.52 mbsf interval is therefore defined by 52.80-01, 0.726±0.052 Ma. 52.80B-01 and 52.80C-01, do not help constrain the age of deposition, but nonetheless provide useful information for provenance studies.

3.3. 85-01 (85.27-85.87 mbsf)

Data from 37 of 39 euhedral sanidine and anorthoclase phenocrysts separated from the 85.27–85.87 mbsf phonolite lapilli tuff (Pompilio et al., 2007) yield a precise inverse isochron age of 1.014 ±0.008 Ma. The sample grains, both single crystal and groups of two to three crystals were fused using the CO_2 laser system. The data form a unimodal normal distribution with a weighted mean age of 1.034 ± 0.004 Ma (MSWD=1.16 Fig. 4A), after rejecting 6 statistically older analyses. Radiogenic yields for individual analyses display significant variation from 35.0-98.8%, but with an average of 81.1±14.3(1σ)%. K/Ca ratios demonstrate a similar spread in value, 0.7-33.9 and an average of

19.5±9.0(1σ).

On an inverse isochron plot (Fig. 4C) the 37 data points form a linear array with a $^{40}Ar/^{36}Ar_{intercept}$ =335±12 and inverse isochron age of 1.014±0.008 Ma (MSWD=1.2). The isochron age, however, is sensitive to which data points are included in the age calculations. For example, all 39 analyses yield a significantly younger isochron age of 0.997±0.015 Ma ($^{40}Ar/^{36}Ar_{intercept}$ =372±20, MSWD=3.9, Fig. 4B). The inverse isochron age for the 33 analyses used to calculated the weighted mean age is 1.026±0.010 Ma (MSWD=1.1, Fig. 4D) with a $^{40}Ar/^{36}Ar_{intercept}$ = 312±17. We choose 1.014±0.008 as the most accurate eruption age for this tephra, however, additional work is need to precisely determine the effect of excess ^{40}Ar on this sample.

3.4. Basaltic Tephra

The age-spectra produced by incremental heating of the glass shard samples generally do not yield statistically defined plateau ages, i.e those defined by 3 or more contiguous heating steps, that overlap at 2σ in apparent age and represent >50% of the total $^{39}Ar_K$ released (Harrison 1983). The discordant spectra display a reproducible 'saddle-shape' with old apparent ages at low and high-temperatures (Fig. 5). Of the 25+ analyses conducted, only two (112.51-01 and 136.21-01) yield statistically robust and precise plateau and inverse isochron ages.

3.4.1 112.51-01 (112.02 – 112.97 mbsf)

Analyses 112.51-01, 02, 03 are from a basaltic tephra interval spanning

112.02-112.97 mbsf, consisting of fresh unaltered brown/black glass shards, containing sparse micro-phenocrysts (Fig. 1C). Analysis 136.21-01 is representative of a basaltic tephra from 136.12-137.22 mbsf, comprised of fresh glass shards and feldspar micro-phenocrysts (Fig. 1D).

Incremental furnace heating of 112.51-01 yields the common 'saddle-shaped' spectrum displayed by the basaltic glass samples. However, a statistically robust plateau age of 1.676±0.057 Ma (MSWD=1.85, Fig. 6A) is defined by >89.7% of the $^{39}Ar_K$ released. Radiogenic yields are variable with a minimum of 4.9% for step A (500ºC) and maximum of 83.9% for step G (900ºC). K/Ca ratios for 94.6% of the spectrum show only minor variation (0.16-0.21). An inverse isochron plot of the plateau steps D-I (Fig. 6B) yields a trapped $^{40}Ar/^{36}Ar$ ratio (318.6±21.8) statistically resolvable from the atmospheric value, and a precise isochron age (1.633±0.057 Ma, MSWD=1.05) that is younger than the plateau age, but overlapping at the 95% confidence level (2σ). From the isochron results we infer 112.51-01 contains a significant quantity of excess ^{40}Ar, causing an increase in apparent age by ~30-40 ka and consider the isochron age an accurate eruption age.

Repeat furnace incremental heating of basaltic glass from 112.51-112.62 mbsf (112.51-02, Fig. 6C) yields the reproducible 'saddle-shaped' spectrum displayed by all furnace heated basaltic glasses. No statistically acceptable plateau is defined by analysis 112.51-02, although steps F and G overlap within 2σ uncertainty of the plateau steps F and G of analysis 112.51-01. The K/Ca values for all steps from 112.51-02 are nearly identical to that of 112.51-01 and

display a similar trend, an approximately constant value (~0.2) for much of the

gas released and a pronounced decrease in value for the last high temperature

steps. The radiogenic yields for 112.51-02 are, in general, less than those

displayed by 112.51-01. The critical difference between 112.51-02 and 112.51-

01, other than the lack of a plateau for 112.51-02, is the large discrepancy in

integrated ages, 5.41±0.13 Ma and 2.85±0.10 Ma, respectively.

Basaltic glass samples incrementally heated using the CO_2 laser system

yield similar spectra to the furnace analyses. Laser analyses do not perfectly

mimic the degassing behavior displayed by furnace analyses, most likely

because of thermal gradients caused by heterogeneous laser coupling, but do

show the same general trend of old low and high temperature apparent ages with

a minimum age at ~50% $^{39}Ar_K$ released. For example, analysis 112.51-03 (Fig.

6D) displays apparent ages that progressively decrease in apparent age for the

first 4 heating steps, followed by an increase in apparent age for the last 3 steps.

Radiogenic yields for 112.51-03 are similar to 112.51-01 and 112.51-02, with a

maximum value of 67.9%. Sample weight (51.25 mg), K2O% (0.92%) and total

moles of $^{39}Ar_K$ released (14.14 x 10^{-15} mol) for 112.51-03 are similar to the values

obtained for 112.51-02 (Weight = 55.4 mg, K2O =1.12%, $^{39}Ar_K$ = 18.57 x 10^{-15}

mol). The agreement of these parameters between 112.51-02 and 112.51-03

adds confidence to the validity of direct comparison of laser and furnace spectra.

Note: The ~4 times greater value in total $^{39}Ar_K$ released for 112.51-01 (70.9 x 10^{-15} mol) compared to 112.51-02 and 112.51-03 is the result of different irradiation

times; analysis 112.51-01, 7 hour irradiation versus, 112.51-02,112.51-03,1 hour

irradiation.

The integrated age for 112.51-03 (4.01±0.16 Ma) falls between the integrated ages for 112.51-01 (2.85±0.10 Ma) and 112.51-02 (5.41±0.13 Ma), and demonstrates an additional aspect of non-reproducibility for ^{40}Ar/^{39}Ar basaltic glass analyses.

3.4.2. 136.21-01 (136.12-137.22 mbsf)

Incremental furnace heating of a basaltic glass sample separated from 136.12-137.22 mbsf yields a statistically defined plateau age of 1.725±0.050 Ma (MSWD=1.41 Fig. 6E), representing 92.1% of the ^{39}Ar$_K$ released. Radiogenic yield and K/Ca ratios for 136.21-01 display values and trends similar to 112.51-01. As with 112.51-01, a plot of the 136.21-01 plateau steps on an inverse isochron (Fig. 6F) yields a ^{40}Ar/^{36}Ar intercept (316.5±17.2) statistically distinguishable from atmosphere and a precise isochron age (1.683±0.055 Ma, MSWD=0.55) younger than the plateau age, but overlapping at 2σ. The elevated ^{40}Ar/^{36}Ar ratio suggests that excess ^{40}Ar has a significant effect on the age of this sample. Therefore, we use the isochron age as our preferred eruption age for 136.21-01.

3.4.3. Basaltic Glass Microprobe Results

Quantitative geochemical and qualitative morphological data for the basaltic glass shard samples were obtained by Electron Microprobe analysis (Appendix B. Table 1). Primary goals for sample characterization at this scale were 1) to

ensure sample homogeneity, 2) identify alteration and or glass hydration, 3)

qualitatively assess the amount of reworking based on grain morphology and 4)

ensure that the sample preparation process adequately removed contaminants

such as clay minerals.

3.5. 481.80-01 (480.97-481.96 mbsf)

Single-crystal laser-fusion analysis of feldspar grains separated from a

pumice clast in a pumice-rich mudstone interval spanning 480.97-481.96 mbsf

mbsf yield a precise weighted mean age of 4.800 ±0.076 Ma (Fig. 4E). The

weighted mean age is statistically robust, indicated by a unimodal normal

distribution of ages and a mean square weighted deviation close to unity (MSWD

=0.74). Analyses 481.80-01-2, 9 and 14 are statistical outliers omitted from

mean age calculations. Analysis 481.80-01-2 yields an age statistically younger

than the mean. The low radiogenic yield (53.4%) and K/Ca (0.79), in addition,

suggest 481.80-01-2 is an altered or low potassium grain. Analysis 481.80-01-9

yields an older age than the weighted mean, but a similar radiogenic yield and

K/Ca. We infer this analysis to represent an older inherited grain. Analysis

481.80-01-14 has an anomalously low $^{39}Ar_K$ signal (0.001 x10^{-15} mol), a $^{40}Ar/^{39}Ar$

ratio (1424.0) inconsistent with the rest of the data set (30.7$_{MEAN}$), and an

anomalously old age (221.6±52.4 Ma). We consider 481.80-01-14 is an altered

or xenocrystic grain. The K/Ca values for all analyses used in the mean age

calculation exhibit significant variability, ranging from 1.1 to 28.5 (Appendix B.

Table 2). This variability in K/Ca, however, does not exceed typical

anorthoclase-sanidine values (Deer et al., 1966).

3.6. 648.36-01 (646.49 – 649.30 mbsf)

Incremental heating in the furnace of a groundmass sample separated from the interior of a intermediate lava flow spanning the interval of 646.49 – 649.30 mbsf yields a moderately robust plateau age of 6.48±0.13 Ma (Fig. 2E). The radiogenic yields for this sample are variable, ranging from 8.0 to 71.9%. However, all of the plateau steps display radiogenic yields >40%, with the maximum value in the approximate middle of the plateau. K/Ca values for the plateau temperature steps all fall in the range of 0.1 to 0.5, typical of plagioclase (Deer et al., 1966). The final high-temperature steps display the decrease in K/Ca characteristic of basaltic groundmass samples. Electron microprobe sample characterization supports the interpretation of the K/Ca spectrum, indicating that the lava consists of a K-rich glassy groundmass containing abundant calcic plagioclase micro-phenocrysts with K-bearing rims and mafic micro-phenocrysts such as pyroxene and/or magnetite (Fig 1E).

An inverse isochron plot for this sample yields a low-precision isochron age of 6.6±0.22 Ma (MSWD =2.74, Fig 3C), statistically equivalent to the plateau age. In addition, the isochron indicates the sample does not have a significant excess ^{40}Ar component ($^{40}Ar/^{36}Ar_{intercept}$ = 288.9±13.8). From the isochron results, we infer that excess ^{40}Ar does not have a measurable effect on the apparent age of the sample and use the plateau as our preferred eruption age.

3.7. 822.78B-01 (822.78-822.80 mbsf)

Incremental heating of a large kaersutite phenocryst separated from a volcanic clast at 822.78-822.80 mbsf yields a plateau age of 8.53±0.51 Ma

(MSWD=0.70, Fig. 2F) for this interval. The plateau age is defined by 100% of the gas released. The majority of degassing took place over a narrow temperature range from 1050 to 1200°C, a pattern common of amphibole step heating analyses (Lee et al., 1991). The radiogenic yields for the individual steps are variable, displaying an increase from 0.5% for the first step (A, 950° C) to a maximum at 83.5% at step G (1170°C, Appendix A, Table 1.). We consider the plateau age for this sample statistically robust and an accurate maximum depositional age.

3.8. ~1280 mbsf Volcanic Clasts

Single-crystal laser fusion of volcanic feldspar phenocrysts, anorthoclase to sanidine in composition, separated from three volcanic clasts at ~1280 mbsf yield a maximum depositional age of 13.57±0.13 Ma. After failing to find fresh K-rich feldspar phenocrysts in altered pumice from the base of the core we dated three volcanic clasts from near 1280 mbsf in an attempt to determine a maximum depositional age. In contrast to the altered tephra, these volcanic clasts contain large fresh feldspar phenocrysts. Fifteen phenocrysts separated from each of these clasts were individually fused using a CO_2 laser. The analyses from each of these three clasts yield tightly grouped normal age distributions. Weighted mean ages for the three clasts are: 1277.91-01, 13.82±0.09 Ma; 1278.84-01, 13.85±0.18 Ma and 1279.00-01, 13.57±0.13 Ma (Fig. 4F). Radiogenic yields for all crystals analyzed are >90%, typical of high-precision single-crystal feldspar data.

The K/Ca values for samples 1277.91-01 and 1279.00-01 exhibit only minor

intra –sample variability (Appendix A. Table 2). Thirteen out of fifteen feldspars

grains dated from 1277.91-01 yield an average K/Ca value of 25.6±11.2. Sample

1279.00-01 exhibits the same small range in K/Ca values (8.0±2.5) for 14 out of

15 feldspar analyses. In contrast, the K/Ca values for the individual analyses of

sample 1278.84-01 are imprecise and variable, spanning a large range in value

from undefined to >20 000. Ten out of fifteen analyses have near background

^{37}Ar signals, (mean value 1.45 x10^{-5} pA or 7.25 x 10^{-19} mol) and indicate Ca-poor

compostions, suggesting that the ^{39}Ar$_K$/^{37}Ar$_{Ca}$ ratio is a poor representation of

feldspar geochemistry for this sample.

4. Discussion

4.1. Felsic tephra

85-01 represents an analysis of a concentrated interval of felsic pumice

interpreted as a primary tephra deposit and an accurate time-stratigraphic

horizon. The inverse isochron age (1.014±0.008 Ma) obtained by laser fusion

analysis of 33 aliquots represents an accurate and precise eruption age. The

high concentration of pumice and pumice fragments, and preservation of fragile

features such as vesicule walls, suggests rapid deposition of the layer with

limited or no reworking. The absence of a lag between eruption and

emplacement permits the use of the eruption age as an accurate proxy for the

time of deposition.

We believe the weighted mean age of 4.800±0.076 Ma for a population of

feldspar grains separated from a pumice clast represents an accurate and

precise constraint on the time of deposition for the mudstone interval at 480.97-481.96 mbsf. This mudstone interval contains numerous dispersed pumice clasts, and a concentrated zone of pumices up to 0.5 cm in diameter at 481.82-481.84 mbsf. Although the pumice clasts are scattered within the mudstone interval, their fragile nature and restriction to a narrow stratigraphic interval suggests that they were deposited soon after eruption as pyroclastic ejecta, and therefore an eruption age is inferred to closely approximate the time of deposition (McIntosh 2001).

The variation in K/Ca, exhibited by the 11 analyses used to calculated the mean age, and supported by Electron microprobe characterization (Appendix B Table 2) can be accounted for by the analysis of 1) zoned feldspars fragmented upon eruption, 2) feldspars from a chemically zoned magma chamber or 3) xenocrystic feldspars incorporated by a vent clearing eruption. Further geochemical and chronology work on additional pumice clasts from 481.00-482.00 will add increased confidence in age of this unit.

4.2. Lava Flow

The plateau age for analysis 648.37-01 represents an accurate eruption age for the intermediate lava flow at 646.49 – 649.30 mbsf. This subaqueous flow is part of a thick sequence of volcanic and volcaniclastic rocks and is thought to have erupted from a local submarine vent, within 4 km of AND-1B, based on the average distance traveled by lava of similar composition (Walker, 1973). We therefore consider the time of eruption equivalent to the time of

deposition and the plateau age of 6.48±0.13 Ma an accurate depositional age.

4.3. Basaltic Tephra

Analyses 112.51-01 and 136.21-01 yield precise plateau and inverse isochron ages. These analyses, despite displaying the consistent saddle or 'U'-shaped spectrum, produce the youngest and most precise plateau ages of all the basaltic glass analyses. The presence of a small but significant amount of excess ^{40}Ar is inferred from inverse isochron plots and we therefore consider the isochron ages accurate eruption ages.

The 'U'-shaped spectrum, attributed to excess ^{40}Ar (Lanphere and Dalrymple, 1976; McDougall and Harrison, 1999; Wartho et al ., 1996), is commonly associated with low potassium minerals such as plagioclase, amphibole, and clinopyroxene. Excess ^{40}Ar, however, is not abundant in volcanic systems because outgassing provides a release mechanism (Kelley 2002). In addition to excess ^{40}Ar several possible explanations for the 'U'-shaped spectra displayed by basaltic glass shard analyses include: 1) irradiation induced effects, such as ^{39}Ar mobilization (i.e. recoil), 2) presence of older material (inherited argon), 3) K loss caused by alteration and/or hydration, or 4) degassing of residual sample material remaining in the furnace crucible.

The basaltic tephra represent important potential dating targets for the upper <600 m of the drill core because of their abundance and relatively high potassium content. The discordant age spectra commonly produced by the glass analyses, however, do not add confidence in the ^{40}Ar/^{39}Ar ages. Only 2 out of 25+ analyses produced statistically robust plateau and inverse isochron ages,

112.51-01, 136.21-01. Further experimental and microprobe work on the basaltic tephra is needed in order to maximize their potential for constraining the chronostratigraphy of the AND-1B drill core and magmatic history of southern McMurdo Sound.

4.4. Volcanic Clasts

Volcanic clasts have been used, in the absence of primary volcanic tephra, to provide maximum depositional age constraints on their host intervals. Separates of eight clasts, four groundmass concentrates, one kaersutite mineral separate and three single and multi-crystal feldspar analyses, yield accurate maximum depositional ages for four stratigraphic intervals.

In addition to constraining the age-depth model, $^{40}Ar/^{39}Ar$ analyses, in conjunction with bulk and trace element geochemical analyses, can be valuable in determining the provenance of volcanic clasts recovered by AND-1B. Deducing volcanic clast provenances are accomplished by correlating their ages and chemistries to that of local volcanic centers such as Ross Island and Minna Bluff (Fig 7.). As an example, volcanic clast 822.78B can be correlated to Minna Bluff by both chemistry and chronology. Kaersutite phenocrysts separated from lava flows and pyroclastic deposits on Minna Bluff yield ages and K_2O (8.43±0.11 Ma, 1.09% K_2O, 8.57±0.12 Ma, 1.06% K_2O, 8.571±0.082 Ma, 0.95% K_2O, 8.968±0.073 Ma, 1.1% K_2O, Fargo et al., (2008)) overlapping at 2σ to values yielded by 822.78B (8.53±0.51 Ma 0.76% K_2O).

Additional factors make Minna Bluff a likely source of volcanic clasts

preserved in the drill core. These factors include 1) its location south of the drill site and directly in the path of postulated paleo-ice flow paths and 2) its extensive eruptive history and production of volcanic material during the mid to late Miocene period sampled by AND-1B.

Volcanic clast provenances and ages are useful in resolving paleo-flow direction of the Ross Ice Shelf, as well as providing insights into when and how the sources of the clasts, local volcanic centers, influenced ice flow. For example, exposed volcanic outcrops on the eastern tip of Minna Bluff record multiple unconformities, inferred as glacial surfaces of erosion. The ages of these surfaces and duration of overriding glacial ice have been constrained by $^{40}Ar/^{39}Ar$ dating of samples taken from stratigraphically above and below the surfaces at 10.46 - 10.31 Ma and 9.81 - 9.46 Ma (Fargo et al., 2008). Fargo (2008) and Ross (unpublished data) suggest Minna Bluff started as an island located at what is now its eastern 'hook' and was built progressively west towards Mt. Discovery during the late Miocene –Pliocene . AND-1B therefore may record the evolution of the Minna Bluff proto-peninsula (the region between Mt Discovery and Minna Bluff hook) as it grew as a submarine and subaerial volcanic center from the late Miocene to Pliocene.

5. Conclusions

The AND-1B drill core recovered a rich and abundant volcanic record. $^{40}Ar/^{39}Ar$ analysis of the mineral separates and groundmass concentrates separated from volcanic units provide valuable time-stratigraphic pinning points for developing a precise and accurate age-depth model. The paucity of fresh

unaltered primary tephra below ~600 mbsf requires analysis of populations of volcanic clasts to provide the necessary pinning points. Volcanic clasts, however, can only be used to infer a maximum depositional age because of the unknown time lag between eruption age (^{40}Ar/^{39}Ar age) and deposition.

In addition to providing time-stratigraphic pinning points, ^{40}Ar/^{39}Ar analyses on volcanic units preserved in AND-1B will aid in our understanding of the evolution of local volcanic centers and features. A record of the growth of Ross Island and Minna Bluff may be preserved in the AND-1B drillcore. The proximity of Ross Island and Minna Bluff to the drill site and the overlap in ages for the drill core with the known ages of volcanism at these two centers increases the opportunities for using AND-1B to investigate the evolution of Southern McMurdo Sound volcanism into the mid-Miocene.

Future ^{40}Ar/^{39}Ar work will focus on improving the mid-Miocene age-depth model by continuing to analyze sets of volcanic clasts, increasing the resolution of the age-depth model for upper Plio-Pleistocene interval, and advancing our understanding of the Argon degassing behavior of basaltic glass shard samples.

6. Acknowledgements

7. Appendices

Appendix A

Table 1. ^{40}Ar/^{39}Ar results for step-heated samples

Table 2. ^{40}Ar/^{39}Ar results for laser fusion samples

Appendix B

Table 1. Electron microprobe results for basaltic glass shards

Table 2. Electron microprobe results for feldspar phenocrysts

8. References

Armstrong, R., 1978. K-Ar dating: Late Cenozoic McMurdo volcanic group and dry valley glacial history, Victoria Land, Antarctica. New Zealand Journal of Geology and Geophysics, 21(6): 685-698.

Cooper, A.F., Adam, L.J., Coulter, R.F., Eby, G.N. and McIntosh, W.C., 2007. Geology, geochronology and geochemistry of a basanitic volcano, White Island, Ross Sea, Antarctica. Journal of Volcanology and Geothermal Research, 165(3-4): 189-216.

Dalrymple, G.B., Lanphere, M.A. and Pringle, M.S., 1988. Correlation diagrams in ^{40}Ar/^{39}Ar dating: Is there a correct choice. Geophys. Res. Lett, 15(6): 589-591.

Deer, W.A., Howie, R.A., Zussman, J. and others, 1978. An introduction to the rock-forming minerals. Longman London.

Esser, R.P., Kyle, P.R. and McIntosh, W.C., 2004. ^{40}Ar/^{39}Ar dating of the eruptive history of Mount Erebus, Antarctica: volcano evolution. Bulletin of Volcanology, 66(8): 671-686.

Fargo, A.J., McIntosh, W.C., Dunbar, N.W., and Wilch, T.I., 2008, ^{40}Ar/^{39}Ar Geochronology of Minna Bluff, Antarctica: Timing of Mid-Miocene glacial erosional events within the Ross Embayment. American Geophysical Union, Fall Meeting 2008, abstract\# V13C-2127

Harrison, T.M., 1983. Some observations on the interpretation ^{40}Ar/^{39}Ar age spectra. Chemical Geology, 1: 319-338.

Horgan, H., Naish, T., Bannister, S., Balfour, N. and Wilson, G., 2005. Seismic stratigraphy of the Ross Island flexural moat under the McMurdo-Ross Ice Shelf, Antarctica, and a prognosis for stratigraphic drilling. Global Planetary Change, 45: 83-97.

Huntingdon, A., Walker, G., Sanders, A. and Walker, D., 1973. Lengths of Lava Flows: Discussion. Philosophical Transactions for the Royal Society of London. Series A, Mathematical and Physical Sciences, 274(1238): 116-118.

Kelley, S., 2002. Excess argon in K-Ar and Ar-Ar geochronology. Chemical Geology, 188(1-2): 1-22.

Lanphere, M. and Dalrymple, G., 1976. Identification of excess ^{40}Ar by the ^{40}Ar/^{39}Ar age spectrum technique. Earth and Planetary Science Letters, 32(2): 1451-148.

Lee, J., Onstott, T., Cashman, K., Cumbest, R. and Johnson, D., 1991. Incremental heating of hornblende in vacuo; implications for ^{40}Ar/^{39}Ar geochronology and the interpretation of thermal histories. Geology, 19(9): 872-876.

Lewis, A.R., Marchant, D.R., Kowalewski, D.E., Baldwin, S.L. and Webb, L.E., 2006. The age and origin of the Labyrinth, western Dry Valleys, Antarctica: Evidence for extensive middle Miocene subglacial floods and freshwater discharge to the Southern Ocean. Geology, 34(7): 513-516.

Marchant, D.R., Denton, G.H., Swisher, C.C. and Potter, N., 1996. Late Cenozoic Antarctic paleoclimate reconstructed from volcanic ashes in the Dry Valleys region of southern Victoria Land. Bulletin of the Geological Society of America, 108(2): 181-194.

McDougall, I. and Harrison, T.M., 1999. Geochronology and Thermochronology by the ^{40}Ar/^{39}Ar Method. Oxford University Press, USA.

McIntosh, W.C., 2000. ^{40}Ar/^{39}Ar geochronology of tephra and volcanic clasts in CRP-2A, Victoria Land Basin. Terra Antartica, 7: 621-630.

McIntosh W.C., C.R.M., 1994. ^{40}Ar/^{39}Ar geochronology of Middle to Late Cenozoic ignimbrites, mafic lavas, and volcaniclastic rocks in the Quemado Region, New Mexico. New Mexico Geological Society Guidebook, 45: 165-185.

Naish, T. and Powell, R. and Levy, R. and Henrys, S. and Krissek, L. and Niessen, F. and Pompilio, M. and Scherer, R. and Wilson, G. 2007. Synthesis of the Initial Scientific Results of the MIS Project (AND-1B Core), Victoria Land Basin, Antarctica. Terra Antartica Publication.

Nier, A.O., 1950. A redetermination of the relative abundances of the isotopes of carbon, nitrogen, oxygen, argon, and potassium. Physical Review(789-793).

Olmsted, B.W., 2000. ^{40}Ar/^{39}Ar investigations of the Ocate volcanic field, north central New Mexico: MS Thesis, New Mexico Institute of Mining and Technology. Unpublished.

Pompilio, M., Kyle, P., Wilch, T. and Dunbar, N., 2007. MIS ANDRILL SCIENCE TEAM (2007), The volcanic record in the ANDRILL McMurdo Ice Shelf AND-1B drill core, Antarctica: A Keystone in a Changing World-Online Proceedings of the 10th ISAES, edited by AK Cooper and CR Raymond et al., USGS Open-File Report.

Renne, P.R. et al., 1998. Intercalibration of standards, absolute ages and uncertainties in ^{40}Ar/^{39}Ar dating. Chemical Geology, 145(1-2): 117-152.

Sandroni, S. and Talarico, F.M., 2006. Analysis of clast lithologies from CIROS-2 core, New Harbour, Antarctica--Implications for ice flow directions during Plio-Pleistocene time. Palaeogeography, Palaeoclimatology, Palaeoecology, 231(1-2): 215-232.

Steiger, R. and Jäger, E., 1977. Subcommission on geochronology: Convention on the use of decay constants in geo-and cosmochronology. Earth and Planetary Science Letter, 36: 359-362.

Talarico, F. and Sandroni, S., 2007. the ANDRILL-MIS Science Team (2007), Clast provenance and variability in MIS (AND-1B) core and their implications for the paleoclimatic evolution recorded in the Windless Bight-southern McMurdo Sound area (Antarctica). Antarctica: A Keystone in a Changing World-Online Proceedings of the 10 th ISAES X, edited by AK Cooper and CR Raymond et al., USGS Open-File Report, 1047.

Tauxe, L., Gans, P. and Mankinen, E.A., 2004. Paleomagnetism and ^{40}Ar/^{39}Ar ages from volcanics extruded during the Matuyama and Brunhes Chrons near McMurdo Sound, Antarctica. Geochemistry Geophysics Geosystems, 5(6).
Taylor, J.R., 1997. An introduction to error analysis: the study of uncertainties in physical measurements. University Science Books.

Wartho, J., Rex, D. and Guise, P., 1996. Excess argon in amphiboles linked to greenschist facies alteration in the Kamila amphibolite belt, Kohistan island arc system, northern Pakistan; insights from ^{40}Ar/^{39}Ar step-heating and acid leaching experiments. Geological Magazine, 133(5): 595-609.

Wilch, T.I., Lux, D.R., Denton, G.H. and McIntosh, W.C., 1993. Minimal Pliocene-Pleistocene uplift of the dry valleys sector of the Transantarctic Mountains: A key parameter in ice-sheet reconstructions. Geology, 21(9).

Wright-Grassham, A.C., 1987. Volcanic geology, mineralogy, and petrogenesis of the Discovery Volcanic Subprovince, southern Victoria Land, Antarctica, Ph.D Dissertation, New Mexico Institute of Mining and Technology. Unpublished.

9. Figure Captions

Figure 1. A) Secondary Electron image (SE) of a 85-01 feldspar phenocryst. (B-E) Back Scatter Electron (BSE) images of B) 85-01 pumice, C) 112.51-01 and D) 136.21-01 mbsf processed basaltic glass shards and E) 648.37-01 groundmass concentrate of submarine lava flow

Figure 2. ^{40}Ar/^{39}Ar age, K/Ca and radiogenic yield spectra for furnace analysis of A) 17.17-01 groundmass concentrate (gm) from volcanic clast, B,C,D) 52.80A,B,C-01 gm from volcanic clast, E) 648.37-01 gm from interior of ~3m thick submarine lava flow, and F) 822.78B-01 kaersutite phenocryst mineral separate from volcanic clast.

Figure 3. Inverse isochron plots for A) 17.17-01, B) 52.80A-01, and C) 648.37-01. Insets for plots A,B show both x and y intercepts. Isochron age and (^{40}Ar/^{36}Ar)intercept calculated from all temperature steps for A and B, for C only plateau steps used.

Figure 4. ^{40}Ar/^{39}Ar age-probablity with stacked auxillary plots of radiogenic yield, moles of ^{39}Ar, and K/Ca and isochron diagrams for laser fusion of single and groups of 2-3 crystals. A) 85-01 age-probablity with isochrons of total population B) 39 analyses, and 2 subgroups. C) 37 valid analyses, and D) 33 valid analyses (open ellipses omitted). E) 481.80-01 age-probablity diagram. Solid line indicates relative probablity with open circles omitted from age calculation,

dashed line - open circles included in age calculation. F) age-probablity diagrams for 1277-91 (red square), 1278-84 (blue triangle), and 1279-00 (black circle)

Figure 5. A-E Examples of the discordant U-shaped spectrum produced by furnace heating of basaltic glass shards. Note that all of the spectrum display a degassing profile described by old apparent ages for the low temperature steps (600-800°C) followed by a decrease in apparent age to a miminum at ~50% gas released (800-900°C). Further heating (950-1700°C) produces increased apparent ages with a subsequent decrease at higher temperature.

Figure 6. ^{40}Ar/^{39}Ar age spectra and inverse isochron diagrams for furnace and laser heating of basaltic glass shards. 112.51-01 (A) and 136.21-01 (E) are the only analyses to yield statistically defined plateau ages, but display the U-shaped spectrum. The corresponding isochron plots are (B and F, respectively) well constrained and suggest the presence of excess ^{40}Ar. 112.51-02 (C) and 112.51-03 (D) illustrate the reproduciblity of the U-shaped spectrum in both the laser and furnace heating devices.

Figure 7. Age (Ma) vs. depth (mbsf) plot showing ^{40}Ar/^{39}Ar ages used to constrain the age-depth models proposed by Wilson et al. 2007 and this study. Inset shows map of Antarctica and McMurdo Sound adapted from Cooper et al., (2007). Bottom plot displays ages for Southern McMurdo Sound volcanism complied from 1) Armstrong (1978), 2) Cooper et al. (2007), 3) Esser et al. (2004), 4) Fargo in progress, 5) Lewis et al. (2006) ,6) Lawrence in press ,7) Marchant et al. (1996), 8) Ross in progress, 9) Tauxe (2004),10) Wilch et al. (1993), 11) Wright-Grassham (1987). Colors correspond to the colors used on inset map of McMurdo Sound.

Figure 1
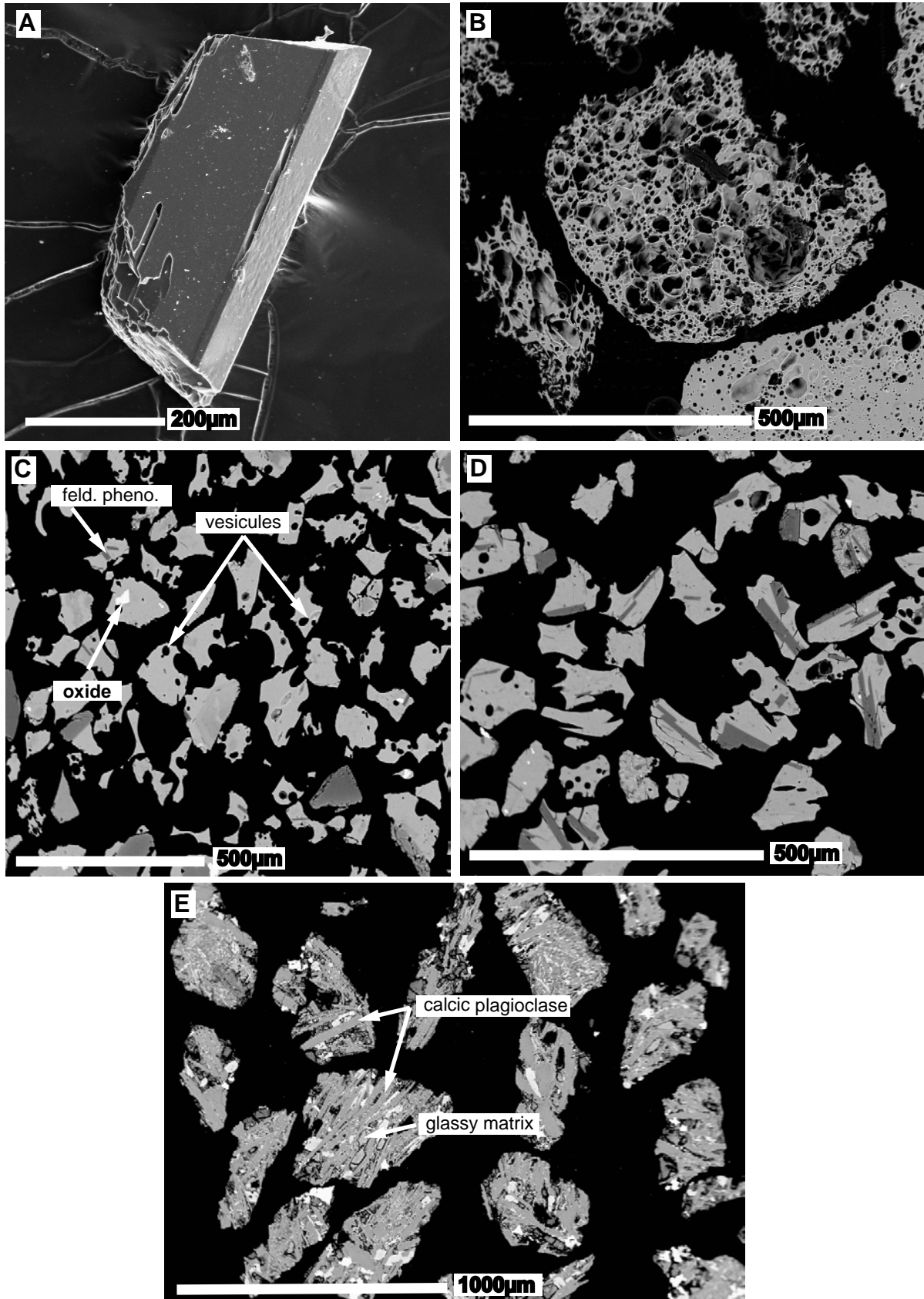
Figure 2
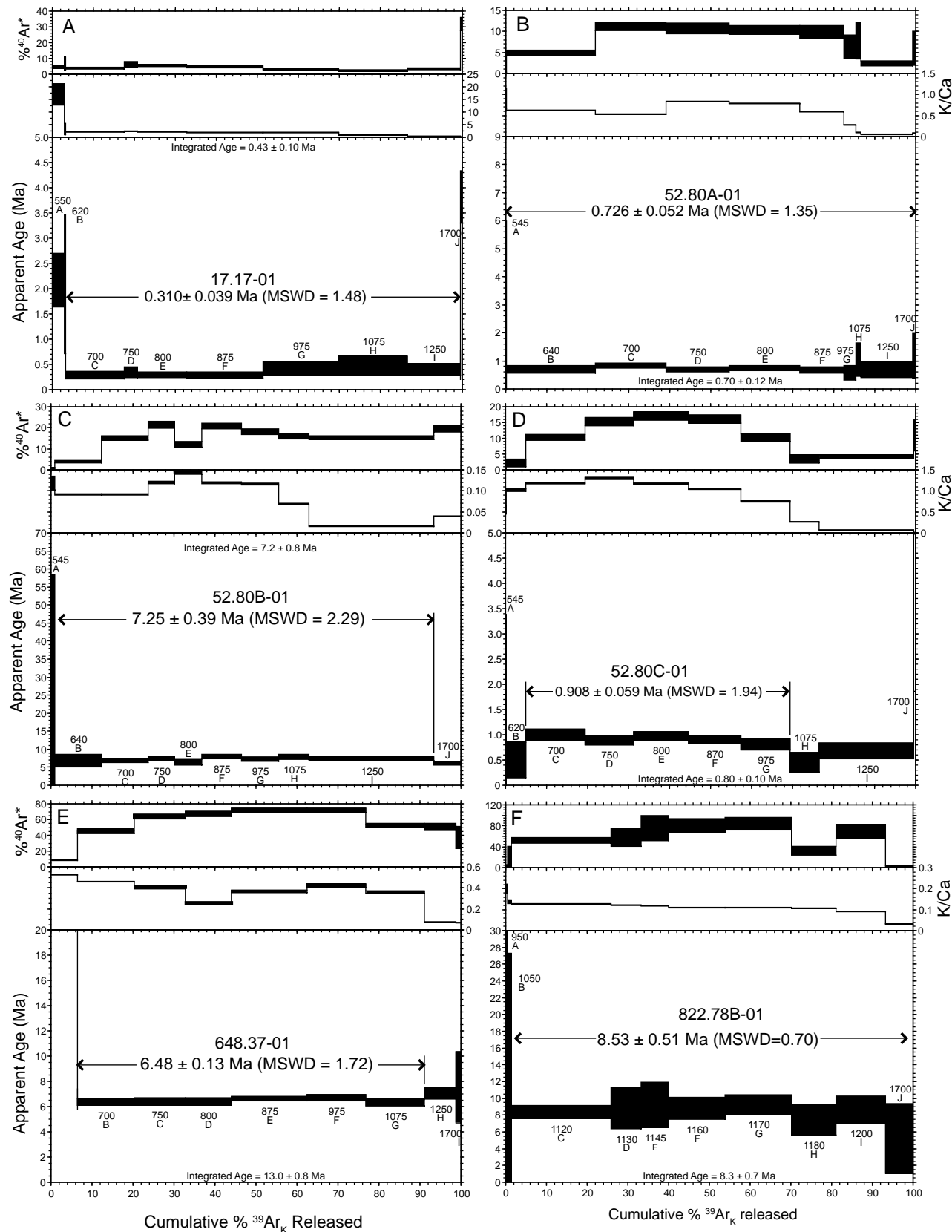
Figure 3
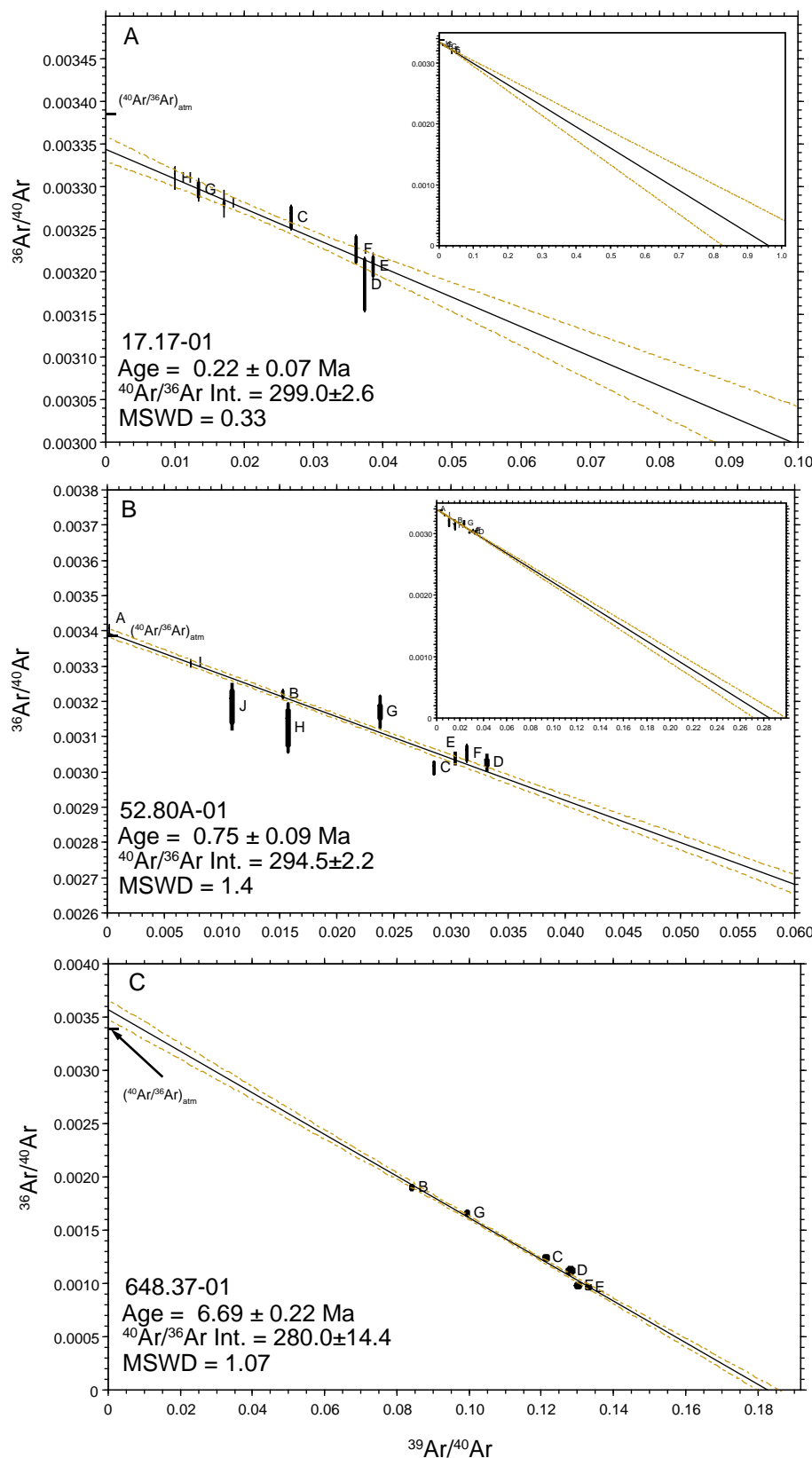
Figure 4
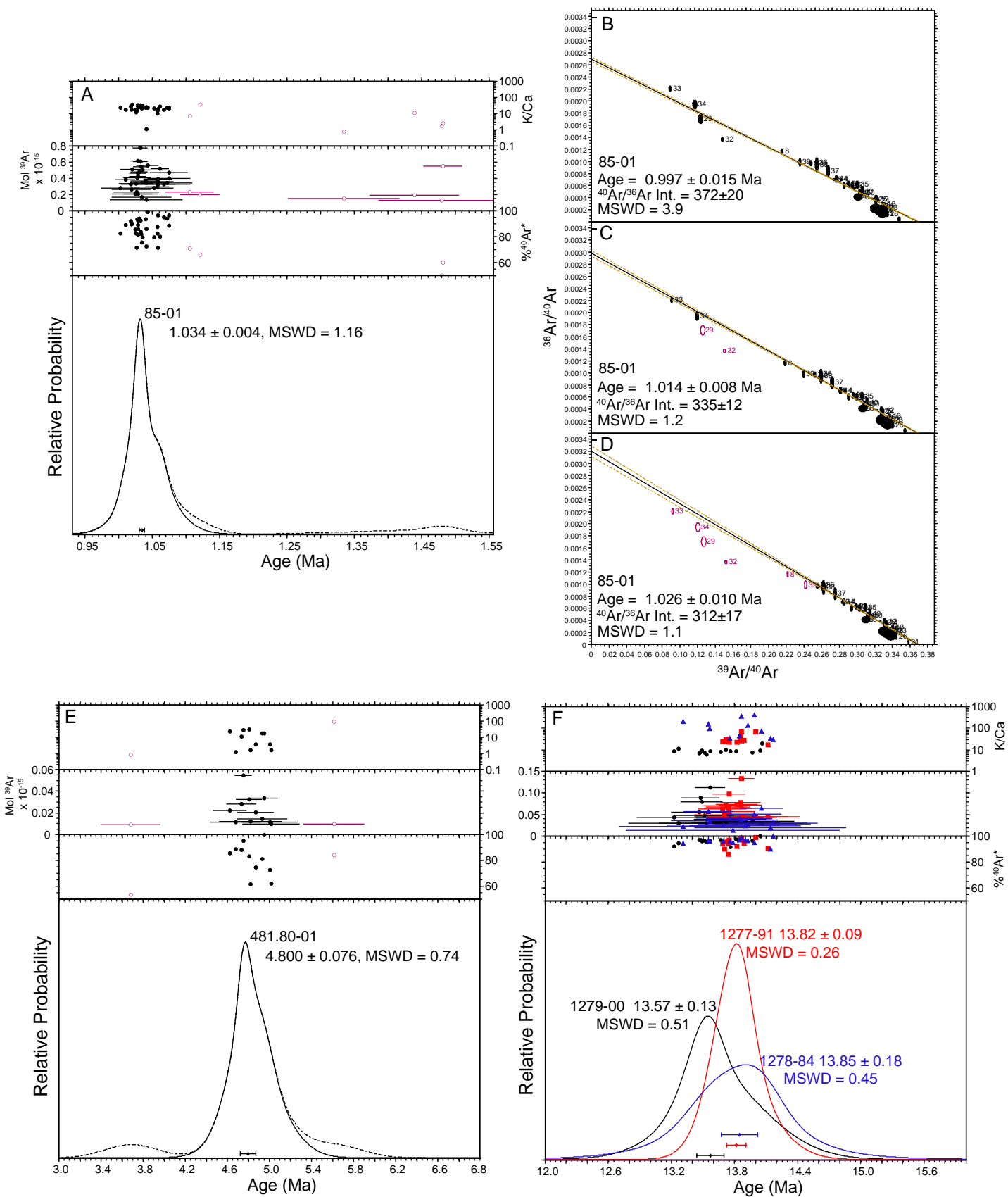
Figure 5

Figure 6

Figure 7

Weddell Sea

Amery Ice Shelf

East Antarctica

West Antarctica

McMurdo Sound

Ross Sea

168°E

Ross Island

Mount Erebus

Hut Point Peninsula

AND-1B

78°S

ice shelf margin

Royal Soc. Range

White Island

Black Island

Ross Ice Shelf

Mount Discovery

Mount Morning

Minna Bluff

Mason Spur

164°E

166°E
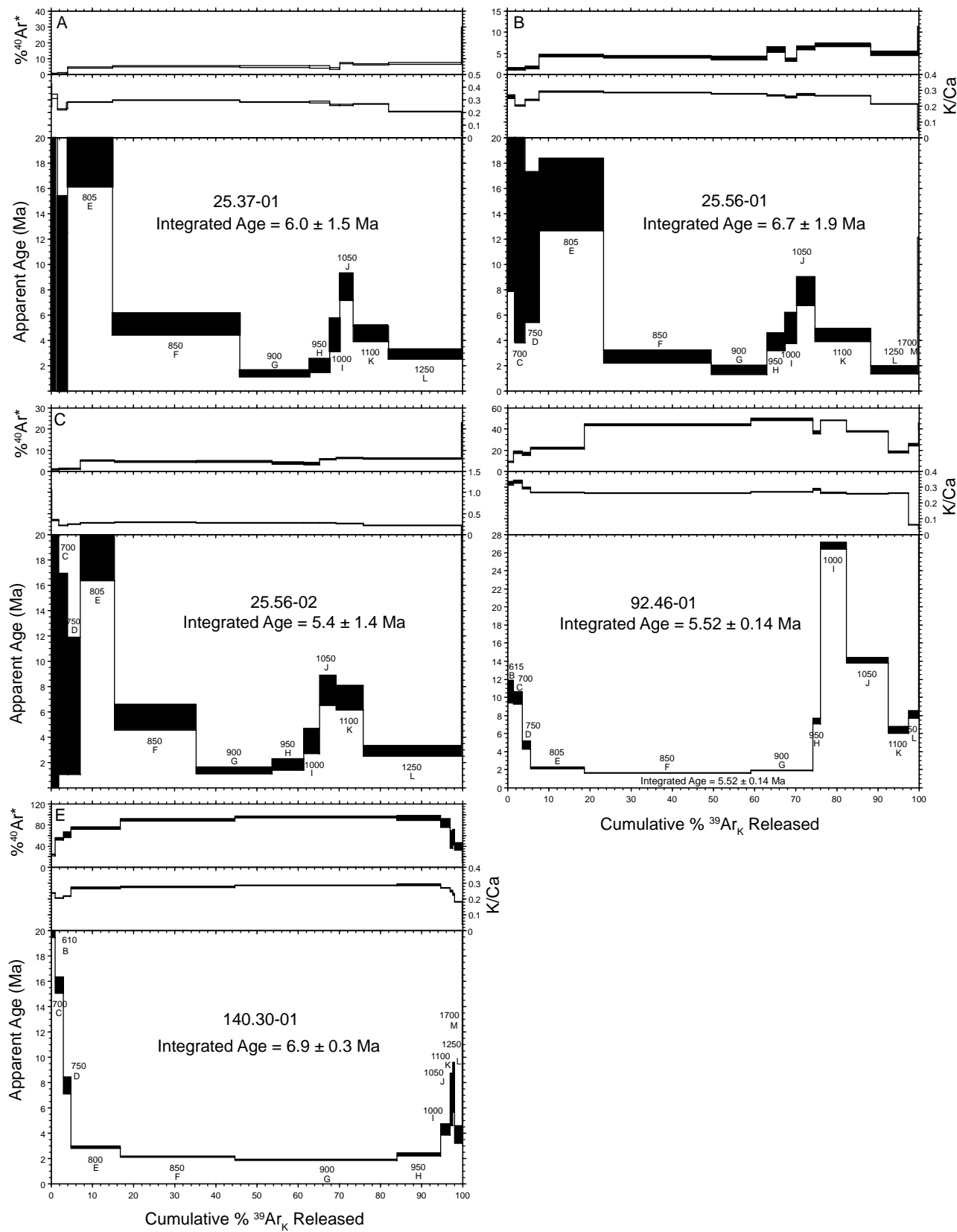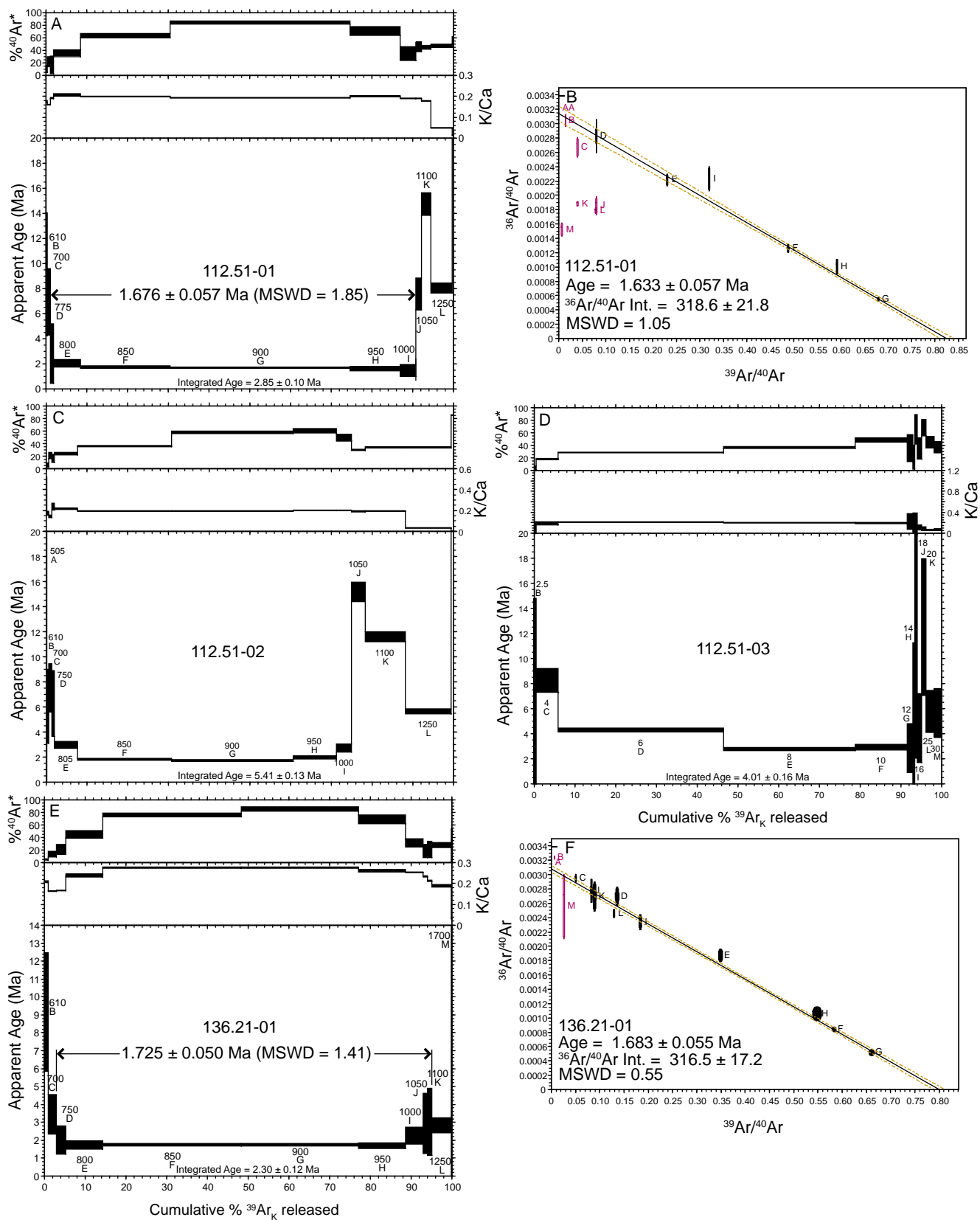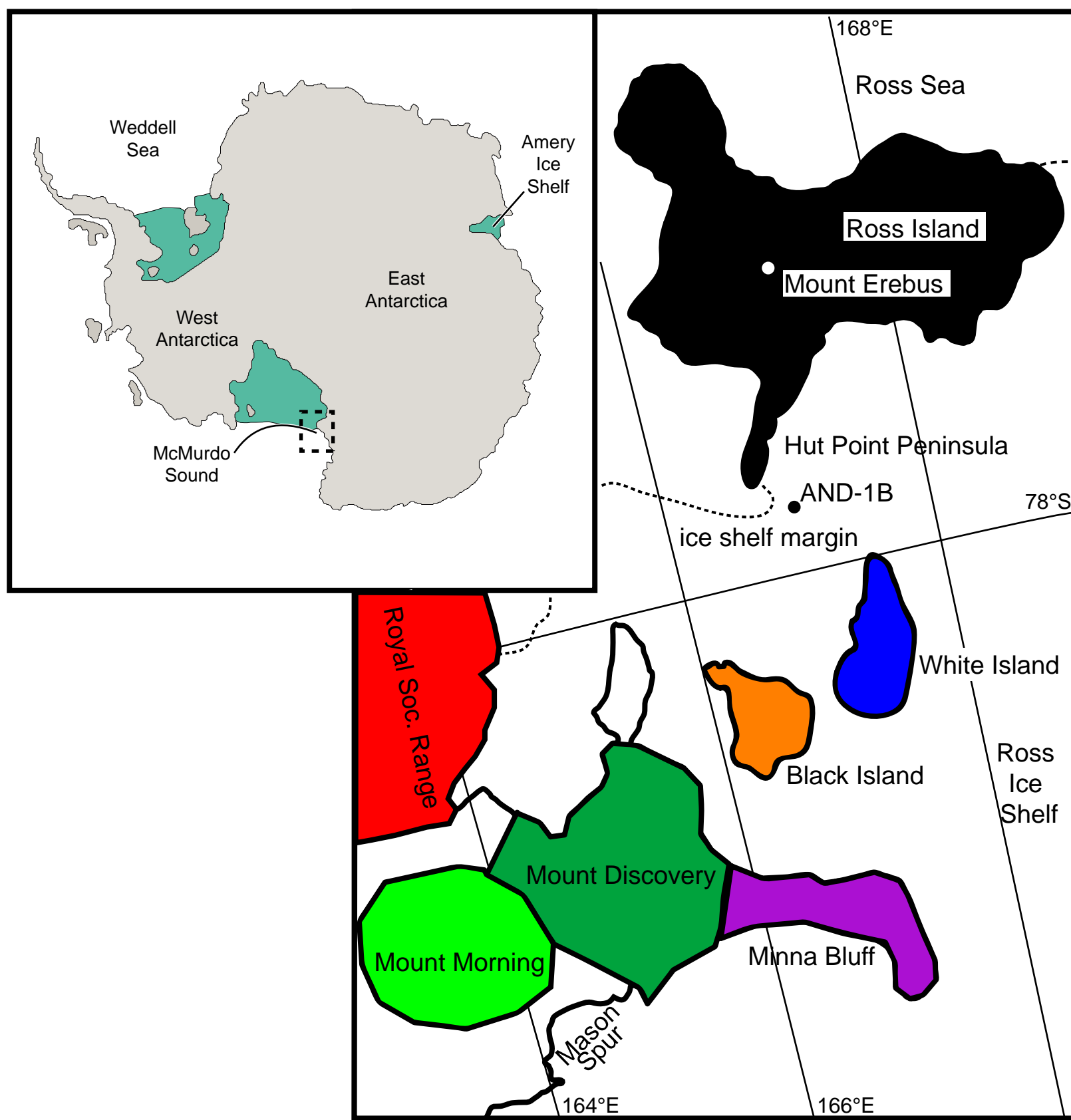
Table 1

Table 1. Summary of $^{40}Ar/^{39}Ar$ results

					Preferred Age					
Sample	Location (mbsf)	L#	Irrad	Material	analysis	n	MSWD	K/Ca ± 2s	Age(Ma)	± 2σ
17.17-01	17.17-17.18	57571	NM-214	GM	Plateau	7	1.48	1.6 ± 1.4	0.310	± 0.039
52.80A-01	52.80-52.82	57573	NM-214	GM	Plateau	10	1.35	0.6 ± 0.7	0.726	± 0.052
85-01	85.27-85.87	56529	NM-198	San/An	Isochron	37	1.2	19.5 ± 18.3	1.014	± 0.004
112.51-01	112.02-112.97	56873	NM-203	Glass	Isochron	6	1.05	0.20 ± 0.01	1.633	± 0.057
136.21-01	136.21-137.22	56867	NM-203	Glass	Isochron	8	0.55	0.26 ± 0.07	1.683	± 0.055
481.80-01	480.97-481.96	57593	NM-214	San/An	Weighted Mean	11	0.7	11.9 ± 20.9	4.80	± 0.076
648.37-01	648.37-648.43	56788	NM-203	GM	Plateau	6	1.7	0.4 ± 0.3	6.48	± 0.13
822.78B-01	822.78-822.80	57845	NM-217	Kaer	Plateau	10	0.7	0.1 ± 0.1	8.53	± 0.51
1277.91-01	1277.91-1277.95	56793	NM-203	San/An	Weighted Mean	15	0.3	31.0 ± 30.4	13.82	± 0.09
1278.84-01	1278.84-1278.97	56794	NM-203	San/An	Weighted Mean	14	0.5	1854.7 ± 11014.7	13.85	± 0.18
1279.00-01	1279.00-1279.04	56792	NM-203	San/An	Weighted Mean	15	0.5	8.7 ± 5.8	13.57	± 0.13

L# = Lab number, Irrad = Irradiation number and tray letter, n = number of analyses use to compute age, MSWD = Mean Square Weighted Deviation
Kaer= kaersutite phenocrysts, Glass= basaltic glass shard concentrate, GM= grondmass concentrate, San/An= sanidine and/or anorthoclase phenocrysts
Notes:
Sample preparation and irradiation:
Basaltic glass shard samples were separated by extensive washing with water followed by an ultrasonic water bath. Sieved and washed samples were
processed in magnetic separator and hand picked to remove additional contaminants. Groundmass concentrates were separated by mechanical crushing
and sieving, followed by magnetic separation to remove phenocrysts, a 5-10 min HCl acid bath, a finally hand picked to ensure sample homogeneity
Feldspar phenocrysts (85-01, 481.80-01, 1277.91-01, 1278.84-01, 1279.00-01) and kaersutite phenocrysts (822.78B), were hand picked using a binocular
 microscope. Samples treated with acid were immersed in 10% HCl or 15% HF in an ultrasonic bath, followed by ultrasonic rinsing with distilled water
 to remove the residual acid.
All samples and neutron flux monitors were loaded into machined Al discs in a known geometry
Neutron flux monitor Fish Canyon Tuff sanidine (FC-2). Assigned age = 28.02 Ma (Renne et al, 1998)

Instrumentation:
Mass Analyzer Products 215-50 mass spectrometer on line with automated all-metal extraction system.
Samples step-heated using a Mo double-vacuum resistance furnace or defocused CO_2 laser. Heating duration in the furnace and laser
were 10 min and 30 sec, respectively.
Reactive gases removed during analysis by reaction with 3 SAES GP-50 getters, 2 operated at ~450°C and
 1 at 20°C. Gas also exposed to a W filament operated at ~2000°C.

Analytical parameters:
Averaged furnace sensitivity 1.24×10^{-16} moles/pA. Averaged laser sensitivity 7.12×10^{-17} moles/pA
Total system blank and background for the furnace averaged 5017, 5.6, 6.5, 29.1, 7.8, 21.7×10^{-18} moles.
Total system blank and background for the laser averaged 376, 5.3, 1.9, 5.6, 7.8, 29.7×10^{-18} moles.
J-factors determined to a precision of ± 0.1% by CO_2 laser-fusion of 4 to 6 single crystals from each of the 6 or 10 radial positions
around the irradiation tray (6 for a 12 hole disc, 10 for a 20 hole disc).
Correction factors for interfering nuclear reactions were determined using K-glass and CaF_2 and are as follows:
   $(^{40}Ar/^{39}Ar)_K$ = 0 ±0.0004; $(^{36}Ar/^{37}Ar)_{Ca}$ = 0.000289±0.000005; and $(^{39}Ar/^{37}Ar)_{Ca}$ = 0.00068±0.00002

Age calculations:
Plateau age or preferred age calculated for the indicated steps by weighting each step by the inverse of the variance.
Plateau age error is inverse-variance-weighted mean error (Taylor, 1982) times root MSWD where MSWD>1.
MSWD values are calculated for n-1 degrees of freedom for plateau age.
Isochron ages, $^{40}Ar/^{36}Ar_i$ and MSWD values calculated from regression results obtained by the methods of York (1969).
Decay constants and isotopic abundances after Steiger and Jäger (1977).

All errors reported at ±2 , unless otherwise noted.

σ

Appendix A

Table 1. $^{40}Ar/^{39}Ar$ analytical data for incremental heating analyses.

	ID	Power/Temp (Watts/°C)	$^{40}Ar/^{39}Ar$	$^{37}Ar/^{39}Ar$	$^{36}Ar/^{39}Ar$ (x 10^{-3})	$^{39}Ar_K$ (x 10^{-15} mol)	K/Ca	$^{40}Ar^*$ (%)	^{39}Ar (%)	Age (Ma)	±1σ (Ma)

17.17-01, Groundmass Concentrate, 67.5 mg, J=0.0001189±0.40%, D=1.001±0.001, NM-214A, Lab#=57571-01

	ID	Power/Temp	$^{40}Ar/^{39}Ar$	$^{37}Ar/^{39}Ar$	$^{36}Ar/^{39}Ar$ (x10^{-3})	$^{39}Ar_K$ (x10^{-15} mol)	K/Ca	$^{40}Ar^*$ (%)	^{39}Ar (%)	Age (Ma)	±1σ (Ma)
xi	A	550	239.6	0.0304	776.8	2.37	16.8	4.2	3.1	2.16	0.27
xi	B	625	149.8	0.1629	474.2	0.142	3.1	6.5	3.2	2.08	0.69
	C	700	37.21	0.2485	121.5	11.12	2.1	3.6	17.6	0.287	0.038
	D	750	26.68	0.2287	85.02	2.50	2.2	5.9	20.8	0.337	0.056
	E	800	25.87	0.2442	83.01	9.4	2.1	5.3	32.9	0.292	0.028
	F	875	27.55	0.2620	88.93	14.4	1.9	4.7	51.4	0.278	0.032
	G	975	74.26	0.2751	244.8	14.3	1.9	2.6	69.9	0.416	0.070
	H	1075	99.53	0.5323	329.5	13.0	0.96	2.2	86.7	0.470	0.093
	I	1250	58.33	1.409	191.7	10.0	0.36	3.1	99.6	0.385	0.060
xi	J	1700	56.23	2.986	131.0	0.338	0.17	31.6	100.0	3.81	0.26
	Integrated age ± 2σ		n=10			77.5	1.1	K2O=3.71%		0.43	0.10
	Plateau ± 2σ	steps C-I	n=7	MSWD=1.48	74.7		1.6 ±1.4		96.3	0.310	0.039
	Isochron±2σ	steps C-I	n=7	MSWD=0.33		$^{40}Ar/^{36}Ar=$	299.0±2.6			0.223	0.071

25.37-01, Glass, 68.8 mg, J=0.0001173±0.36%, D=1.002±0.001, NM-214B, Lab#=57578-01

	ID	Power/Temp	$^{40}Ar/^{39}Ar$	$^{37}Ar/^{39}Ar$	$^{36}Ar/^{39}Ar$ (x10^{-3})	$^{39}Ar_K$ (x10^{-15} mol)	K/Ca	$^{40}Ar^*$ (%)	^{39}Ar (%)	Age (Ma)	±1σ (Ma)
x	A	500	54717.0	1.542	184137.4	0.081	0.33	0.6	0.2	63.4	47.5
x	B	600	8909.3	1.565	30002.9	0.581	0.33	0.5	1.6	9.2	7.8
x	C	700	4838.7	2.289	16267.3	0.94	0.22	0.7	3.8	6.8	4.3
x	D	750	3851.2	2.019	12969.8	0.145	0.25	0.5	4.1	4.0	4.2
x	E	800	2320.0	1.821	7528.2	4.64	0.28	4.1	15.0	20.1	2.0
x	F	850	501.2	1.728	1612.1	13.1	0.30	5.0	45.9	5.28	0.43
x	G	900	134.1	1.831	432.1	7.20	0.28	4.9	62.8	1.39	0.13
x	H	950	204.3	1.828	659.9	2.12	0.28	4.6	67.8	1.99	0.25
x	I	1000	586.3	1.967	1914.0	1.04	0.26	3.6	70.3	4.42	0.64
x	J	1050	560.6	1.975	1766.7	1.40	0.26	6.9	73.5	8.19	0.53
x	K	1100	334.7	1.923	1061.4	3.64	0.27	6.3	82.1	4.48	0.32
x	L	1250	201.0	2.490	634.4	7.50	0.20	6.8	99.8	2.91	0.19
x	M	1700	670.7	34.44	1641.8	0.103	0.015	28.1	100.0	40.4	1.9
	Integrated age ± 2σ		n=13			42.5	0.25	K2O=2.02%		5.9	1.5

25.56-01, Glass, 70.8 mg, J=0.0001174±0.40%, D=1.002±0.001, NM-214B, Lab#=57579-01

	ID	Power/Temp	$^{40}Ar/^{39}Ar$	$^{37}Ar/^{39}Ar$	$^{36}Ar/^{39}Ar$ (x10^{-3})	$^{39}Ar_K$ (x10^{-15} mol)	K/Ca	$^{40}Ar^*$ (%)	^{39}Ar (%)	Age (Ma)	±1σ (Ma)
x	A	500	160499.3	7.432	535093.2	0.066	0.069	1.5	0.1	446.4	163.3
x	B	600	8615.9	1.986	28789.0	0.811	0.26	1.3	1.9	22.9	7.5
x	C	700	4631.6	2.526	15482.7	1.17	0.20	1.2	4.5	12.0	4.1
x	D	750	3411.7	2.138	11364.6	1.55	0.24	1.6	7.8	11.3	3.0
x	E	800	1667.9	1.753	5396.3	7.23	0.29	4.4	23.5	15.5	1.4
x	F	850	310.0	1.792	1006.3	12.0	0.28	4.1	49.7	2.71	0.27
x	G	900	200.8	1.844	653.7	6.21	0.28	3.9	63.2	1.64	0.19
x	H	950	317.0	1.922	1011.3	2.02	0.27	5.8	67.6	3.88	0.34
x	I	1000	670.8	1.985	2191.6	1.33	0.26	3.5	70.4	4.95	0.62
x	J	1050	598.1	1.878	1899.0	2.05	0.27	6.2	74.9	7.86	0.56
x	K	1100	303.0	1.934	955.5	6.23	0.26	6.9	88.4	4.41	0.27
x	L	1250	158.8	2.423	511.9	5.24	0.21	4.9	99.8	1.64	0.16
x	M	1700	498.0	9.767	1554.4	0.076	0.052	7.9	100.0	8.4	1.9
	Integrated age ± 2σ		n=13			46.0	0.26	K2O=2.13%		6.7	1.9

Table 1. continued

ID	Power/Temp (Watts/°C)	$^{40}Ar/^{39}Ar$	$^{37}Ar/^{39}Ar$	$^{36}Ar/^{39}Ar$ (x 10^{-3})	$^{39}Ar_K$ (x 10^{-15} mol)	K/Ca	$^{40}Ar^*$ (%)	^{39}Ar (%)	Age (Ma)	±1σ (Ma)
52.80A-01, Groundmass Concentrate, 64 mg, J=0.000119±0.39%, D=1.002±0.001, NM-214A, Lab#=57573-01										
A	550	4952.9	0.5630	16842.5	0.133	0.91	-0.5	0.3	-5.2	5.6
B	625	65.06	0.8366	209.6	9.84	0.61	4.9	21.9	0.684	0.068
C	700	34.99	0.9603	105.6	7.88	0.53	11.0	39.2	0.829	0.046
D	750	30.09	0.6189	91.22	7.06	0.82	10.6	54.7	0.684	0.047
E	800	32.86	0.6525	99.92	7.82	0.78	10.3	71.8	0.727	0.045
F	875	31.84	0.8764	97.41	4.92	0.58	9.8	82.6	0.671	0.058
G	975	41.89	1.878	133.3	1.36	0.27	6.3	85.6	0.57	0.13
H	1075	62.89	5.216	197.9	0.525	0.098	7.7	86.7	1.04	0.30
I	1250	135.9	9.527	452.0	5.71	0.054	2.3	99.3	0.68	0.14
J	1700	90.77	6.247	290.7	0.330	0.082	5.9	100.0	1.16	0.40
Integrated age ± 2σ		n=10			45.6	0.25	K2O=2.30%		0.70	0.12
Plateau ± 2σ	steps A-J	n=10	MSWD=1.35		45.6	0.57 ±0.65		100.0	0.726	0.052
Isochron±2σ	steps A-J	n=10	MSWD=1.41			$^{40}Ar/^{36}Ar$=	294.5±2.2		0.752	0.072
52.80B-01, Groundmass Concentrate, 57.3 mg, J=0.0001187±0.40%, D=1.002±0.001, NM-214A, Lab#=57574-01										
A	550	18356.8	4.327	61765.9	0.093	0.12	0.6	1.0	22.5	17.9
B	625	843.4	5.588	2750.3	1.03	0.091	3.7	12.4	6.68	0.87
C	700	209.5	5.643	604.4	1.03	0.090	15.0	23.9	6.74	0.30
D	750	160.6	4.290	428.9	0.582	0.12	21.3	30.4	7.33	0.30
E	800	248.1	3.605	740.9	0.600	0.14	11.9	37.0	6.31	0.41
F	875	177.2	4.282	476.6	0.883	0.12	20.7	46.8	7.88	0.29
G	975	186.4	4.424	518.1	0.827	0.12	18.0	56.0	7.21	0.29
H	1075	228.6	7.533	653.5	0.665	0.068	15.8	63.4	7.76	0.36
xi I	1250	216.7	31.39	630.4	2.71	0.016	15.2	93.5	7.20	0.26
xi J	1700	145.0	12.99	399.8	0.589	0.039	19.2	100.0	6.01	0.27
Integrated age ± 2σ		n=10			9.01	0.037	K2O=0.51%		7.23	0.80
Plateau ± 2σ	steps A-H	n=8	MSWD=2.29		5.71	0.10 ±0.05		63.4	7.25	0.39
Isochron±2σ	steps A-H	n=8	MSWD=2.57			$^{40}Ar/^{36}Ar$=	295.5±2.2		7.25	0.39
52.80C-01, Groundmass Concentrate, 58 mg, J=0.0001185±0.35%, D=1.002±0.001, NM-214A, Lab#=57575-01										
xi A	550	2696.8	0.9421	9189.3	0.135	0.54	-0.7	0.3	-4.0	3.7
xi B	625	113.3	0.5019	375.8	2.24	1.0	2.0	5.0	0.49	0.18
C	700	45.75	0.4332	139.2	6.90	1.2	10.1	19.6	0.992	0.058
D	750	27.13	0.3957	77.92	5.57	1.3	15.2	31.3	0.884	0.044
E	800	26.59	0.4367	74.82	6.36	1.2	17.0	44.7	0.966	0.044
F	875	26.05	0.4897	74.17	6.12	1.0	16.0	57.6	0.893	0.039
G	975	37.34	0.6847	113.9	5.65	0.75	10.0	69.5	0.802	0.057
xi H	1075	62.29	1.951	204.3	3.35	0.26	3.4	76.6	0.449	0.099
xi I	1250	75.98	8.226	248.8	10.9	0.062	4.1	99.6	0.674	0.080
xi J	1700	142.4	45.52	442.1	0.192	0.011	10.9	100.0	3.41	0.78
Integrated age ± 2σ		n=10			47.4	0.20	K2O=2.65%		0.80	0.10
Plateau ± 2σ	steps C-G	n=5	MSWD=1.94		30.6	1.1 ±0.4		64.5	0.908	0.059
Isochron±2σ	steps C-G	n=5	MSWD=2.52			$^{40}Ar/^{36}Ar$=	297.0±8.4		0.88	0.16

Table 1. continued

	ID	Power/Temp	$^{40}Ar/^{39}Ar$	$^{37}Ar/^{39}Ar$	$^{36}Ar/^{39}Ar$	$^{39}Ar_K$	K/Ca	$^{40}Ar*$	^{39}Ar	Age	±1σ
		(Watts/°C)			(x 10⁻³)	(x 10⁻¹⁵ mol)		(%)	(%)	(Ma)	(Ma)

92.46-01, Glass, 60.1 mg, J=0.0001168±0.36%, D=1.002±0.001, NM-214B, Lab#=57581-01

	ID	Power/Temp	$^{40}Ar/^{39}Ar$	$^{37}Ar/^{39}Ar$	$^{36}Ar/^{39}Ar$	$^{39}Ar_K$	K/Ca	$^{40}Ar*$	^{39}Ar	Age	±1σ
x	A	500	22162.3	3.826	74620.7	0.027	0.13	0.5	0.1	23.5	24.8
x	B	600	581.0	1.583	1795.6	0.677	0.32	8.7	1.5	10.62	0.64
x	C	700	265.6	1.540	739.5	0.98	0.33	17.8	3.6	9.93	0.35
x	D	750	139.0	1.749	395.3	0.98	0.29	16.1	5.7	4.70	0.23
x	E	800	46.75	1.922	124.3	6.12	0.27	21.8	18.7	2.144	0.055
x	F	850	17.50	1.953	33.79	19.1	0.26	43.9	59.2	1.619	0.018
x	G	900	18.29	1.910	32.26	7.06	0.27	48.7	74.2	1.879	0.023
x	H	950	95.53	1.804	206.1	0.89	0.28	36.4	76.1	7.32	0.16
x	I	1000	266.7	1.951	471.2	2.95	0.26	47.9	82.4	26.73	0.20
x	J	1050	178.3	1.994	377.1	4.76	0.26	37.6	92.6	14.08	0.14
x	K	1100	168.1	1.968	466.9	2.31	0.26	18.0	97.5	6.37	0.20
x	L	1250	155.3	8.098	398.0	1.14	0.063	24.7	99.9	8.11	0.22
x	M	1700	701.2	13.34	1361.3	0.047	0.038	42.8	100.0	62.7	4.5
	Integrated age ± 2σ			n=13		47.0	0.24	K2O=2.57%		5.52	0.14

112.51-01, Glass, 53.08 mg, J=0.0007472±0.07%, D=1.002±0.001, NM-203P, Lab#=56873-01

	ID	Power/Temp	$^{40}Ar/^{39}Ar$	$^{37}Ar/^{39}Ar$	$^{36}Ar/^{39}Ar$	$^{39}Ar_K$	K/Ca	$^{40}Ar*$	^{39}Ar	Age	±1σ
xi	A	500	26808.6	3.023	86309.4	0.006	0.17	4.9	0.0	1229.4	222.7
xi	B	600	66.82	2.911	204.0	0.221	0.18	10.1	0.4	9.1	2.4
xi	C	700	24.25	3.208	65.59	0.386	0.16	21.2	1.2	6.9	1.3
	D	750	12.44	2.668	35.87	0.404	0.19	16.6	2.0	2.8	1.2
	E	800	4.312	2.470	10.20	3.35	0.21	34.8	8.5	2.03	0.16
	F	850	2.041	2.575	3.292	11.38	0.20	62.8	30.6	1.730	0.049
	G	900	1.468	2.660	1.542	22.7	0.19	83.9	74.8	1.663	0.025
	H	950	1.686	2.571	2.410	6.32	0.20	70.4	87.1	1.602	0.077
	I	1000	3.117	2.718	7.691	1.97	0.19	34.3	90.9	1.44	0.23
xi	J	1050	12.37	2.711	23.70	0.695	0.19	45.2	92.3	7.54	0.64
xi	K	1100	24.53	2.868	46.76	1.175	0.18	44.6	94.6	14.73	0.45
xi	L	1250	12.52	10.43	25.24	2.70	0.049	47.3	99.8	8.02	0.21
xi	M	1700	123.9	40.11	199.1	0.098	0.013	55.2	100.0	92.4	5.2
	Integrated age ± 2σ			n=13		51.4	0.16	K2O=0.50%		2.846	0.098
	Plateau ± 2σ	steps D-I		n=6	MSWD=1.85	46.1	0.20 ±0.01		89.7	1.676	0.057
	Isochron±2σ	steps D-I		n=6	MSWD=1.05		$^{40}Ar/^{36}Ar=$	318.6±21.8		1.633	0.057

112.51-02, Glass, 55.4 mg, J=0.0001151±0.35%, D=1.002±0.001, NM-214C, Lab#=57584-01

	ID	Power/Temp	$^{40}Ar/^{39}Ar$	$^{37}Ar/^{39}Ar$	$^{36}Ar/^{39}Ar$	$^{39}Ar_K$	K/Ca	$^{40}Ar*$	^{39}Ar	Age	±1σ
x	A	500	12214.7	1.490	40945.0	0.031	0.34	0.9	0.2	23.9	15.1
x	B	600	519.5	3.030	1660.7	0.103	0.17	5.6	0.7	6.0	1.5
x	C	700	175.4	3.637	472.1	0.151	0.14	20.6	1.5	7.51	0.96
x	D	750	188.8	2.180	537.6	0.101	0.23	16.0	2.1	6.3	1.3
x	E	800	61.08	2.414	159.5	1.06	0.21	23.2	7.8	2.94	0.13
x	F	850	24.51	2.603	54.14	4.30	0.20	35.6	30.9	1.816	0.038
x	G	900	14.26	2.635	21.28	5.54	0.19	57.4	60.7	1.704	0.028
x	H	950	15.51	2.578	21.65	1.98	0.20	60.1	71.4	1.941	0.055
x	I	1000	26.26	2.566	45.74	0.692	0.20	49.3	75.1	2.69	0.16
x	J	1050	247.9	2.672	592.2	0.624	0.19	29.5	78.5	15.15	0.38
x	K	1100	165.9	2.685	373.5	1.84	0.19	33.6	88.4	11.57	0.20
x	L	1250	80.86	14.92	186.7	2.08	0.034	33.3	99.6	5.64	0.10
x	M	1700	1883.6	105.9	993.4	0.081	0.005	84.9	100.0	326.5	11.1
	Integrated age ± 2σ			n=13		18.6	0.11	K2O=1.12%		5.41	0.13

Table 1. continued

	ID	Power/Temp (Watts/°C)	$^{40}Ar/^{39}Ar$	$^{37}Ar/^{39}Ar$	$^{36}Ar/^{39}Ar$ (x 10^{-3})	$^{39}Ar_K$ (x 10^{-15} mol)	K/Ca	$^{40}Ar^*$ (%)	^{39}Ar (%)	Age (Ma)	±1σ (Ma)
112.51-03, Glass, 51.25 mg, J=0.0001151±0.35%, D=1.004±0.001, NM-214C, Lab#=57584-02										
x	A	2	18339.9	7.950	61685.6	0.005	0.064	0.6	0.0	23.3	143.7
x	B	3	913.9	5.271	2981.1	0.077	0.097	3.7	0.6	6.9	3.9
x	C	4	229.7	2.866	644.3	0.744	0.18	17.2	5.8	8.21	0.48
x	D	6	74.33	2.569	182.7	5.76	0.20	27.7	46.6	4.273	0.073
x	E	8	36.65	2.648	79.90	4.57	0.19	36.2	78.9	2.757	0.054
x	F	10	29.02	2.756	51.68	1.80	0.19	48.2	91.6	2.91	0.11
x	G	12	39.09	2.374	86.83	0.195	0.21	34.9	93.0	2.83	0.97
x	H	14	117.4	3.303	315.6	0.074	0.15	20.8	93.5	5.1	3.1
x	I	16	87.04	3.171	103.9	0.079	0.16	65.0	94.1	11.7	4.9
x	J	18	61.15	5.077	136.4	0.157	0.10	34.8	95.2	4.4	1.4
x	K	20	88.91	6.386	99.77	0.147	0.080	67.4	96.2	12.5	2.7
x	L	25	61.71	8.875	118.1	0.289	0.057	44.6	98.3	5.75	0.83
x	M	30	74.89	8.053	164.1	0.245	0.063	36.1	100.0	5.65	0.97
	Integrated age ± 2σ		n=13			14.1	0.17	K2O=0.92%		4.00	0.16
114.44-01, Glass, 59.48 mg, J=0.0002092±0.10%, D=1.002±0.001, NM-198M, Lab#=56533-01										
x	A	2	1977.0	0.7658	6658.7	0.119	0.67	0.5	0.1	3.6	3.5
x	B	3	305.5	1.173	1015.6	0.726	0.43	1.8	1.0	2.07	0.60
x	C	4	110.1	1.956	337.1	2.82	0.26	9.6	4.5	4.00	0.18
x	D	6	42.02	2.203	112.6	7.65	0.23	21.3	14.7	3.377	0.060
x	E	8	22.04	2.281	51.44	10.67	0.22	31.9	30.8	2.656	0.032
x	F	10	18.63	2.352	35.62	10.35	0.22	44.6	49.2	3.136	0.026
x	G	12	15.42	2.441	29.41	10.62	0.21	45.0	71.6	2.620	0.022
x	H	14	11.94	2.796	12.90	6.13	0.18	70.0	86.6	3.158	0.019
x	I	17	11.52	3.008	17.06	1.81	0.17	58.4	91.3	2.544	0.047
x	J	20	17.12	2.887	31.88	1.019	0.18	46.4	94.1	2.998	0.092
x	K	25	16.14	3.215	28.20	0.992	0.16	50.0	96.8	3.051	0.080
x	L	30	16.93	3.475	28.83	1.13	0.15	51.4	100.0	3.289	0.075
	Integrated age ± 2σ		n=12			54.1	0.21	K2O=1.67%		2.987	0.088
114.44-02, Glass, 36.33 mg, J=0.0002098±0.10%, D=1.002±0.001, NM-198M, Lab#=56530-03										
X	A	3	476.6	1.122	1601.4	0.549	0.45	0.7	1.2	1.30	0.83
X	B	4	106.1	1.911	319.7	2.97	0.27	11.1	7.7	4.46	0.18
X	C	6	36.97	2.232	97.82	7.17	0.23	22.3	24.1	3.124	0.055
X	D	0	21.05	2.309	50.13	8.60	0.22	30.5	45.2	2.437	0.045
X	E	10	15.15	2.397	31.77	6.90	0.21	39.3	63.4	2.259	0.028
X	F	12	14.17	2.422	29.81	5.08	0.21	39.2	77.5	2.106	0.035
X	G	14	17.58	2.447	38.67	3.43	0.21	36.1	87.5	2.408	0.038
X	H	20	15.07	2.806	30.48	2.73	0.18	41.8	95.8	2.384	0.038
X	I	25	16.29	3.234	37.42	1.38	0.16	33.8	100.0	2.084	0.064
	Integrated age ± 2σ		n=9			38.8	0.22	K2O=1.96%		2.609	0.093
114.44-03, Glass, 51.9 mg, J=0.0001145±0.39%, D=1.002±0.001, NM-214C, Lab#=57585-01										
	A	500	22834.8	22.21	74704.1	0.011	0.023	3.3	0.0	151.1	84.4
	B	600	941.4	3.471	3061.2	0.097	0.15	3.9	0.5	7.7	8.9
	C	700	186.9	3.161	547.1	0.187	0.16	13.6	1.3	5.3	4.6
	D	750	124.5	2.286	369.2	0.189	0.22	12.5	2.1	3.2	4.6
	E	800	53.25	2.298	145.4	1.51	0.22	19.7	8.6	2.17	0.58
	F	850	17.76	2.457	31.95	6.10	0.21	48.0	34.8	1.76	0.14
	G	900	13.73	2.504	19.80	6.76	0.20	58.9	63.8	1.67	0.13

Table 1. continued

	ID	Power/Temp (Watts/°C)	$^{40}Ar/^{39}Ar$	$^{37}Ar/^{39}Ar$	$^{36}Ar/^{39}Ar$ (x 10^{-3})	$^{39}Ar_K$ (x 10^{-15} mol)	K/Ca	$^{40}Ar*$ (%)	^{39}Ar (%)	Age (Ma)	±1σ (Ma)
		114.44-03. continued									
	H	950	15.64	2.483	23.25	2.33	0.21	57.4	73.9	1.86	0.37
	I	1000	45.62	2.523	115.8	0.73	0.20	25.5	77.0	2.4	1.2
xi	J	1050	234.3	2.555	565.0	0.616	0.20	28.8	79.6	13.9	1.4
xi	K	1100	160.8	2.509	411.4	2.07	0.20	24.5	88.5	8.15	0.45
xi	L	1250	68.76	9.110	173.0	2.64	0.056	26.7	99.9	3.82	0.34
xi	M	1700	920.0	71.17	1184.6	0.034	0.007	62.6	100.0	120.9	25.9
	Integrated age ± 2σ		n=13			23.3	0.15	K2O=1.50%		3.23	0.28
	Plateau ± 2σ	steps A-I	n=9	MSWD=0.69	17.9	0.21 ±0.13			77.0	1.74	0.18
	Isochron±2σ	steps A-I	n=9	MSWD=0.12		$^{40}Ar/^{36}Ar=$	306.3±9.5			1.68	0.19
		114.44-04, Glass, 50.43 mg, J=0.0001145±0.39%, D=1.004±0.001, NM-214C, Lab#=57585-02									
x	A	2	891.1	5.996	3064.1	0.098	0.085	-1.5	0.4	-2.9	2.3
x	B	3	475.1	4.494	1612.7	0.273	0.11	-0.2	1.6	-0.21	0.94
x	C	4	181.7	2.411	510.2	1.87	0.21	17.1	9.6	6.43	0.22
x	D	5	63.58	2.438	154.7	4.26	0.21	28.4	27.8	3.736	0.074
x	E	6	34.54	2.420	71.98	8.96	0.21	39.0	68.5	2.785	0.034
x	F	8	42.09	2.515	94.36	4.40	0.20	34.2	87.3	2.981	0.057
x	G	10	28.84	2.755	56.52	1.08	0.19	42.9	91.9	2.56	0.17
x	H	15	31.84	3.426	68.24	0.779	0.15	37.6	95.3	2.48	0.24
x	I	20	33.13	5.693	69.02	0.593	0.090	39.9	97.8	2.74	0.32
x	J	25	53.83	8.125	142.0	0.331	0.063	23.3	99.2	2.60	0.57
x	K	30	112.5	9.470	322.6	0.180	0.054	16.0	100.0	3.7	1.1
	Integrated age ± 2σ		n=11			23.4	0.19	K2O=1.56%		3.21	0.11
		136.21-01, Glass, 53.3 mg, J=0.0007416±0.07%, D=1.002±0.001, NM-203O, Lab#=56867-01									
xi	A	500	27907.0	2.833	88181.7	0.009	0.18	6.6	0.0	1560.0	267.2
xi	B	600	154.0	2.468	498.9	0.596	0.21	4.4	0.7	9.1	1.7
xi	C	700	19.68	3.164	58.82	1.200	0.16	13.0	2.0	3.42	0.55
	D	750	7.283	3.097	20.49	1.46	0.16	20.4	3.6	1.99	0.39
	E	800	2.857	2.169	5.955	5.54	0.24	44.7	10.1	1.71	0.11
	F	850	1.710	1.853	1.943	20.7	0.28	75.4	38.4	1.726	0.030
	G	900	1.511	1.852	1.288	17.6	0.28	85.0	69.2	1.719	0.034
	H	950	1.817	1.968	2.474	7.08	0.26	68.7	84.0	1.672	0.080
	I	1000	5.431	2.030	13.25	2.62	0.25	31.0	89.9	2.25	0.24
	J	1050	12.05	2.193	34.01	0.661	0.23	18.1	91.4	2.92	0.84
	K	1100	11.08	2.421	30.54	0.613	0.21	20.4	92.8	3.02	0.94
xi	L	1250	7.699	2.715	19.67	2.92	0.19	27.4	99.8	2.83	0.21
xi	M	1700	38.21	16.49	102.0	0.074	0.031	24.7	100.0	12.7	7.4
	Integrated age ± 2σ		n=13			61.1	0.25	K2O=0.59%		2.30	0.11
	Plateau ± 2σ	steps D-K	n=8	MSWD=1.41	56.3	0.26 ±0.07			92.1	1.725	0.050
	Isochron±2σ	steps D-K	n=8	MSWD=0.55		$^{40}Ar/^{36}Ar=$	316.5±17.2			1.683	0.055
		140.30-01, Glass, 48.9 mg, J=0.0007407±0.05%, D=1.002±0.001, NM-203O, Lab#=56868-01									
x	A	500	59733.6	3.381	179334.7	0.028	0.15	11.3	0.0	3233.7	204.8
x	B	600	69.82	2.159	182.4	0.631	0.24	23.1	1.1	21.43	1.00
x	C	700	21.98	2.523	35.31	1.177	0.20	53.5	2.9	15.67	0.33
x	D	750	9.471	2.358	13.04	1.225	0.22	61.4	4.9	7.76	0.33
x	E	800	2.928	1.905	3.160	7.46	0.27	73.5	16.8	2.877	0.051
x	F	850	1.793	1.860	1.150	17.4	0.27	89.6	44.7	2.149	0.025
x	G	900	1.477	1.795	0.7633	24.7	0.28	94.8	84.1	1.872	0.019
x	H	950	1.846	1.776	0.9324	6.59	0.29	93.0	94.6	2.296	0.055
x	I	1000	3.856	1.903	2.749	1.52	0.27	83.0	97.1	4.28	0.22
x	J	1050	9.515	2.061	15.97	0.321	0.25	52.2	97.6	6.6	1.0
x	K	1100	10.11	2.234	15.55	0.356	0.23	56.4	98.1	7.61	1.00
x	L	1250	7.442	2.859	16.20	1.090	0.18	38.9	99.9	3.87	0.35
x	M	1700	36.66	12.14	95.09	0.072	0.042	26.1	100.0	12.8	4.6
	Integrated age ± 2σ		n=13			62.6	0.27	K2O=0.66%		6.93	0.30

Table 1. continued

	ID	Power/Temp (Watts/°C)	$^{40}Ar/^{39}Ar$	$^{37}Ar/^{39}Ar$	$^{36}Ar/^{39}Ar$ (x 10^{-3})	$^{39}Ar_K$ (x 10^{-15} mol)	K/Ca	$^{40}Ar^*$ (%)	^{39}Ar (%)	Age (Ma)	±1σ (Ma)
	145.16-01, Glass, 48 mg, J=0.0007429±0.06%, D=1.002±0.001, NM-203O, Lab#=56870-10										
	1A	2	788.5	1.482	2661.1	0.426	0.34	0.3	0.4	3.0	8.2
	1B	3	64.91	2.251	211.2	2.52	0.23	4.2	2.5	3.62	0.88
	1C	4	10.01	1.946	29.17	33.4	0.26	15.5	32.0	2.08	0.25
	1E	8	4.575	1.858	10.59	41.2	0.27	34.9	72.0	2.144	0.031
xi	1F	10	3.720	1.747	8.540	7.25	0.29	36.1	79.5	1.799	0.048
xi	1G	12	4.423	1.879	10.22	6.24	0.27	35.3	86.1	2.092	0.046
xi	1H	14	5.230	2.039	13.27	3.19	0.25	28.2	89.4	1.981	0.085
xi	1I	17	5.771	1.887	14.42	2.22	0.27	28.9	91.8	2.24	0.10
xi	1J	20	6.106	2.409	15.41	2.45	0.21	28.7	94.5	2.35	0.10
xi	1K	25	5.373	2.430	13.85	3.40	0.21	27.6	98.2	1.987	0.080
xi	1L	30	10.52	2.826	30.41	1.68	0.18	16.8	100.0	2.37	0.20
	Integrated age ± 2σ		n=11			104.0	0.26	K2O=1.12%		2.14	0.20
	Plateau ± 2σ	steps A-E	n=4	MSWD=0.97	77.5	0.27 ±0.10		74.6		2.14	0.06
	Isochron±2σ	steps A-E	n=4	MSWD=0.97		$^{40}Ar/^{36}Ar=$	297.4±3.7			2.118	0.081
	145.16-02, Glass, 59.46 mg, J=0.0007429±0.06%, D=1.002±0.001, NM-203O, Lab#=56870-01										
x	A	500	38346.1	5.303	125303.9	0.010	0.096	3.4	0.0	1235.6	280.5
x	B	600	147.9	2.099	458.4	1.134	0.24	8.5	1.2	16.9	1.4
x	C	700	22.50	2.635	59.40	2.18	0.19	23.0	3.5	6.92	0.44
x	D	750	12.02	2.835	30.83	1.579	0.18	26.2	5.2	4.23	0.46
x	E	800	4.424	2.113	9.555	9.94	0.24	40.1	15.5	2.382	0.081
x	F	850	3.395	1.809	7.023	30.7	0.28	43.3	46.3	1.970	0.032
x	G	900	2.282	1.757	3.434	33.8	0.29	61.9	78.3	1.894	0.025
x	H	950	2.733	1.878	4.106	12.09	0.27	61.3	89.3	2.247	0.066
x	I	1000	5.932	1.970	10.96	3.59	0.26	48.1	92.6	3.83	0.21
x	J	1050	16.59	2.180	43.41	0.907	0.23	23.8	93.4	5.29	0.80
x	K	1100	17.29	2.260	48.73	1.049	0.23	17.8	94.3	4.13	0.75
x	L	1250	11.24	2.833	29.40	6.20	0.18	24.8	99.9	3.74	0.16
x	M	1700	103.6	14.91	273.1	0.146	0.034	23.3	100.0	32.3	5.5
	Integrated age ± 2σ		n=13			103.3	0.26	K2O=0.90%		2.75	0.11
	145.16-03, Glass, 55.8 mg, J=0.0001141±0.39%, D=1.002±0.001, NM-214C, Lab#=57586-01										
x	A	500	16494.4	15.95	54352.4	0.012	0.032	2.6	0.0	88.2	46.4
x	B	600	769.7	2.061	1850.8	0.210	0.25	29.0	0.5	45.4	2.5
x	C	700	346.3	2.429	701.5	0.363	0.21	40.2	1.4	28.5	1.4
x	D	750	200.7	2.311	389.8	0.090	0.22	42.7	1.6	17.6	5.7
x	E	800	82.74	1.996	171.7	1.48	0.26	38.9	5.3	6.62	0.36
x	F	850	37.89	1.865	78.42	3.99	0.27	39.3	17.3	3.06	0.14
x	G	900	22.93	1.836	38.09	5.6	0.28	51.6	41.5	2.435	0.094
x	H	950	27.23	1.843	32.11	2.37	0.28	65.7	56.0	3.68	0.22
x	I	1000	60.72	1.859	81.05	0.74	0.27	60.8	61.2	7.59	0.70
x	J	1050	284.1	1.935	761.1	0.300	0.26	20.9	63.5	12.2	1.7
x	K	1100	220.3	1.951	683.4	0.99	0.26	8.4	71.5	3.82	0.58
x	L	1250	100.5	3.387	284.7	2.76	0.15	16.6	99.6	3.44	0.21
x	M	1700	589.3	21.48	841.9	0.035	0.024	58.1	100.0	70.1	14.8
	Integrated age ± 2σ		n=13			18.9	0.24	K2O=1.14%		4.87	0.23
	145.16-04, Glass, 51.18 mg, J=0.0001141±0.39%, D=1.004±0.001, NM-214C, Lab#=57586-02										
x	A	2	644.9	5.059	2200.3	0.168	0.10	-0.8	0.5	-1.0	1.4
x	B	3	532.9	3.438	1545.5	0.482	0.15	14.4	2.0	15.7	1.2
x	C	4	244.2	2.223	636.5	1.98	0.23	23.0	8.2	11.56	0.27
x	D	5	108.1	1.906	301.9	4.09	0.27	17.7	21.0	3.93	0.11
x	E	6	59.75	1.836	158.1	13.4	0.28	22.0	64.2	2.713	0.049
x	F	8	32.01	1.877	59.35	6.08	0.27	45.7	84.5	3.012	0.042
x	G	10	40.89	1.944	88.28	2.31	0.26	36.6	92.3	3.082	0.092
x	H	15	41.73	2.350	97.76	1.90	0.22	31.3	98.8	2.69	0.11
x	I	20	65.85	3.483	139.5	0.250	0.15	37.8	99.7	5.13	0.89
x	J	25	663.4	4.366	2051.1	0.056	0.12	8.7	99.9	11.9	7.1
x	K	30	439.3	3.027	1297.1	0.041	0.17	12.8	100.0	11.6	9.6
	Integrated age ± 2σ		n=11			30.7	0.26	K2O=2.02%		3.76	0.13

Table 1. continued

ID	Power/Temp (Watts/°C)	$^{40}Ar/^{39}Ar$	$^{37}Ar/^{39}Ar$	$^{36}Ar/^{39}Ar$ (x 10^{-3})	$^{39}Ar_K$ (x 10^{-15} mol)	K/Ca	$^{40}Ar*$ (%)	^{39}Ar (%)	Age (Ma)	±1σ (Ma)
648.37-01, Groundmass Concentrate, 51.89 mg, J=0.0006793±0.10%, D=1.002±0.001, NM-203C, Lab#=56788-01										
xi A	625	1088.4	0.9775	3389.9	2.81	0.52	8.0	9.5	103.3	4.9
B	700	11.85	1.117	22.82	5.96	0.46	43.9	27.7	6.36	0.13
C	750	8.227	1.282	10.53	5.35	0.40	63.5	42.3	6.39	0.13
D	800	7.788	2.099	9.292	4.83	0.24	67.0	54.1	6.39	0.15
E	875	7.500	1.409	7.533	7.89	0.36	71.9	71.4	6.600	0.093
F	975	7.666	1.225	7.839	6.16	0.42	71.1	83.2	6.67	0.12
G	1075	10.03	1.443	17.02	6.12	0.35	51.1	93.9	6.28	0.13
xi H	1250	11.60	7.004	21.88	3.32	0.073	49.3	99.3	7.02	0.22
xi I	1700	16.60	7.771	37.67	0.469	0.066	36.8	100.0	7.5	1.4
Integrated age ± 2σ			n=9		42.9	0.27	K2O=0.47%		13.03	0.73
Plateau ± 2σ steps B-G			n=6	MSWD=1.72	36.3	0.37 ±0.15		84.6	6.48	0.13
Isochron±2σ steps B-G			n=6	MSWD=1.07		$^{40}Ar/^{36}Ar=$	280.0±14.4		6.69	0.22
822.78A, Kaer, 19.09 mg, J=0.0008199±0.19%, D=1.004±0.001, NM-217K, Lab#=57844-01										
xi A	950	160.9	2.516	437.9	0.085	0.20	19.7	0.2	46.3	15.1
B	1050	95.57	4.362	216.0	0.019	0.12	33.6	0.3	47.0	63.2
C	1120	62.87	4.312	187.3	0.153	0.12	12.6	0.6	11.7	8.5
D	1130	35.68	4.795	107.3	0.242	0.11	12.3	1.2	6.5	5.1
E	1145	10.41	4.828	14.02	0.657	0.11	64.0	2.8	9.9	1.9
F	1150	9.086	4.842	11.84	1.10	0.11	65.9	5.5	8.9	1.1
G	1160	8.474	4.905	9.254	3.14	0.10	72.5	13.1	9.10	0.41
H	1200	6.625	4.885	3.217	29.6	0.10	91.8	85.2	8.998	0.066
xi I	1700	29.92	4.900	83.99	6.07	0.10	18.4	100.0	8.15	0.35
Integrated age ± 2σ			n=9		41.1	0.10	K2O=1.01%		8.98	0.23
Plateau ± 2σ steps B-H			n=7	MSWD=0.16	34.9	0.10 ±0.01		85.0	9.00	0.13
Isochron±2σ steps B-H			n=7	MSWD=0.20		$^{40}Ar/^{36}Ar=$	299.7±39.7		8.99	0.16
822.78B, Kaer, 8.18 mg, J=0.0008194±0.14%, D=1.004±0.001, NM-217K, Lab#=57845-01										
A	950	498.8	2.568	1680.5	0.067	0.20	0.5	0.5	3.5	20.4
B	1050	46.15	3.730	136.1	0.136	0.14	13.5	1.5	9.2	9.0
C	1120	10.86	4.088	18.82	3.23	0.12	51.9	25.9	8.34	0.40
D	1130	10.53	4.236	16.64	0.980	0.12	56.6	33.3	8.8	1.2
E	1145	8.260	4.377	8.145	0.911	0.12	75.2	40.1	9.2	1.4
F	1160	7.469	4.663	6.503	1.84	0.11	79.4	54.0	8.78	0.67
G	1170	7.470	4.696	5.477	2.16	0.11	83.5	70.3	9.23	0.58
H	1180	15.77	4.795	37.75	1.45	0.11	31.8	81.2	7.41	0.93
I	1200	8.502	5.704	10.63	1.61	0.089	68.6	93.3	8.64	0.79
J	1700	158.3	16.22	528.6	0.882	0.031	2.2	100.0	5.2	2.1
Integrated age ± 2σ			n=10		13.3	0.095	K2O=0.76%		8.35	0.67
Plateau ± 2σ steps A-J			n=10	MSWD=0.70	13.3	0.11 ±0.08		100.0	8.53	0.51
Isochron±2σ steps A-J			n=10	MSWD=0.37		$^{40}Ar/^{36}Ar=$	290.8±5.1		8.69	0.52

Notes:
Power refers to laser watts (2-30W), Temp refers to requested furnace temperature (500-1700°C).
Isotopic ratios corrected for blank, radioactive decay, and mass discrimination, not corrected for interfering reactions.
Errors quoted for individual analyses include analytical error only, without interfering reaction or J uncertainties.
Integrated age calculated by summing isotopic measurements of all steps.
Integrated age error calculated by quadratically combining errors of isotopic measurements of all steps.
Plateau age is inverse-variance-weighted mean of selected steps.
Plateau age error is inverse-variance-weighted mean error (Taylor, 1982) times root MSWD where MSWD>1.
Plateau error is weighted error of Taylor (1982).
Decay constants and isotopic abundances after Steiger and Jäger (1977).
x symbol preceding sample ID denotes analyses excluded from plateau age calculations, xi exclusion from plateau and isochron
Weight percent K$_2$O calculated from ^{39}Ar signal, sample weight, and instrument sensitivity.
Ages calculated relative to FC-2 Fish Canyon Tuff sanidine interlaboratory standard at 28.02 Ma
Decay Constant (LambdaK (total)) = 5.543e-10/a
Correction factors:
$(^{39}Ar/^{37}Ar)_{Ca}$ = 0.00068 ± 2e-05
$(^{36}Ar/^{37}Ar)_{Ca}$ = 0.00028 ± 1e-05
$(^{38}Ar/^{39}Ar)_K$ = 0.013
$(^{40}Ar/^{39}Ar)_K$ = 0 ± 0.0004

Table 2. ^{40}Ar/^{39}Ar analytical data for laser fusion analyses.

ID	^{40}Ar/^{39}Ar	^{37}Ar/^{39}Ar	^{36}Ar/^{39}Ar (x 10^{-3})	^{39}Ar$_K$ (x 10^{-15} mol)	K/Ca	^{40}Ar* (%)	Age (Ma)	±1σ (Ma)
85-01, J=0.0002099±0.09%, D=1.002±0.001, NM-198M, Lab#=56529								
35	3.229	0.0226	1.962	2.751	22.5	82.1	1.004	0.024
12	3.006	0.0319	1.133	3.784	16.0	89.0	1.011	0.011
13	2.938	0.0193	0.8327	3.217	26.4	91.7	1.018	0.011
25	3.019	0.0312	1.113	2.597	16.4	89.2	1.019	0.025
24	2.999	0.0151	1.030	5.054	33.9	89.9	1.021	0.013
40	3.176	0.0297	1.595	2.075	17.2	85.2	1.025	0.031
42	3.298	0.0462	2.000	3.300	11.0	82.2	1.026	0.021
36	3.816	0.0359	3.741	2.258	14.2	71.1	1.027	0.030
23	2.910	0.0298	0.6673	4.014	17.1	93.3	1.028	0.016
10	3.167	0.0189	1.509	4.586	27.0	86.0	1.029	0.008
06	2.948	0.0183	0.7669	4.208	28.0	92.4	1.029	0.009
09	3.343	0.0162	2.102	2.076	31.5	81.5	1.029	0.018
01	3.065	0.0163	1.162	6.098	31.3	88.8	1.029	0.007
02	2.916	0.0178	0.6408	4.783	28.6	93.6	1.031	0.008
03	3.267	0.0203	1.817	7.746	25.1	83.6	1.033	0.007
14	2.959	0.0155	0.7684	6.039	32.9	92.4	1.033	0.007
11	3.354	0.0235	2.103	5.370	21.7	81.5	1.034	0.008
37	3.631	0.0267	3.042	1.632	19.1	75.3	1.035	0.041
04	3.448	0.0175	2.404	4.970	29.1	79.4	1.035	0.010
43	2.939	0.0238	0.6539	3.657	21.5	93.5	1.040	0.018
38	3.808	0.5014	3.721	1.321	1.0	72.2	1.041	0.050
45	3.204	0.0215	1.539	3.400	23.7	85.9	1.041	0.020
21	2.791	0.0238	0.1225	5.558	21.4	98.8	1.044	0.012
44	3.508	0.0247	2.464	2.725	20.6	79.3	1.053	0.025
07	3.199	0.0520	1.374	2.927	9.8	87.4	1.058	0.013
41	3.400	0.0359	2.059	3.540	14.2	82.2	1.058	0.020
22	3.916	0.0273	3.792	3.266	18.7	71.4	1.059	0.022
26	2.906	0.0308	0.3733	3.858	16.5	96.3	1.059	0.017
05	3.533	0.0193	2.456	5.158	26.4	79.5	1.062	0.009
27	2.978	0.0301	0.5403	3.242	16.9	94.7	1.068	0.035
30	3.021	0.0238	0.6450	3.411	21.4	93.8	1.072	0.034
31	2.954	0.0246	0.3938	4.675	20.7	96.1	1.075	0.025
28	3.223	0.0240	1.304	3.937	21.3	88.1	1.075	0.029
39	4.126	0.0751	4.094	2.272	6.8	70.8	1.106	0.032
08	4.515	0.0151	5.241	1.928	33.7	65.7	1.122	0.025
34	8.270	0.7157	16.25	1.502	0.71	42.6	1.336	0.079
33	10.88	0.0479	23.96	1.905	10.6	35.0	1.440	0.062
x 29	7.853	0.3218	13.43	1.260	1.6	49.8	1.481	0.089
x 32	6.559	0.2176	9.005	5.481	2.3	59.7	1.483	0.025
Mean age ± 2σ	n=37	MSWD=3.09			20.4 ±16.7		1.036	0.008
481.80-01, J=0.0001131±0.30%, D=1.002±0.001, NM-214D, Lab#=57593								
x 02	33.89	0.6435	53.63	0.078	0.79	53.4	3.69	0.25
06	26.68	0.0242	13.40	0.190	21.1	85.2	4.63	0.13
03	26.11	0.4535	10.70	0.097	1.1	88.0	4.68	0.21
13	26.51	0.0503	11.01	0.242	10.2	87.7	4.74	0.12
01	24.66	0.0192	4.419	0.474	26.5	94.7	4.759	0.055
05	28.46	0.0179	16.40	0.279	28.5	83.0	4.811	0.098
11	38.69	0.3320	50.94	0.103	1.5	61.2	4.82	0.27
12	32.21	0.1424	28.08	0.176	3.6	74.3	4.87	0.15
10	30.07	0.0307	19.76	0.125	16.6	80.6	4.94	0.21
04	24.47	0.0311	0.5258	0.289	16.4	99.4	4.95	0.10
07	34.00	0.1463	31.88	0.099	3.5	72.3	5.01	0.24
08	40.05	0.3436	52.22	0.079	1.5	61.5	5.02	0.24
x 09	32.84	0.0059	17.79	0.082	86.2	84.0	5.62	0.27
x 14	1424.0	0.1898	908.9	0.006	2.7	81.1	221.6	26.2
Mean age ± 2σ	n=11	MSWD=0.74			11.9 ±20.9		4.800	0.076

Table 2. continued

ID	$^{40}Ar/^{39}Ar$	$^{37}Ar/^{39}Ar$	$^{36}Ar/^{39}Ar$ (x 10^{-3})	$^{39}Ar_K$ (x 10^{-15} mol)	K/Ca	Cl/K	$^{40}Ar^*$ (%)	Age (Ma)	±1σ (Ma)
1277.91-01, Sanidine, J=0.0007122±0.04%, D=1. 02±0.001, NM-203D, Lab#=56793									
15	11.43	0.0220	2.502	1.386	23.2	0.000	93.5	13.69	0.20
01	11.91	0.0224	4.060	1.081	22.8	0.000	89.9	13.71	0.26
13	11.24	0.0182	1.762	1.536	28.1	0.000	95.4	13.72	0.18
07	11.40	0.0189	2.265	1.490	27.0	0.000	94.1	13.74	0.19
03	12.56	0.0168	6.165	1.416	30.3	0.000	85.5	13.75	0.20
06	11.15	0.0236	1.404	1.237	21.6	0.000	96.3	13.75	0.22
12	11.10	0.0223	1.234	2.162	22.9	0.000	96.7	13.75	0.13
08	11.78	0.0234	3.344	1.626	21.8	0.000	91.6	13.82	0.17
14	11.08	0.0184	0.8519	1.709	27.8	0.000	97.7	13.86	0.16
09	11.05	0.0128	0.7312	1.573	39.9	0.000	98.1	13.86	0.18
04	11.09	0.0078	0.8702	0.949	65.5	0.000	97.7	13.87	0.29
11	11.09	0.0212	0.8559	2.949	24.0	0.000	97.7	13.869	0.097
05	11.49	0.0194	2.165	0.968	26.3	-0.001	94.4	13.90	0.29
02	11.09	0.0076	0.4978	0.974	66.8	0.000	98.7	14.01	0.28
10	12.24	0.0310	4.118	0.996	16.5	0.000	90.1	14.12	0.28
Mean age ± 2σ	n=15	MSWD=0.26			31.0 ±30.4			13.816	0.096
1278.84-01, Sanidine, J=0.0007111±0.04%, D=1.002±0.001, NM-203D, Lab#=56794									
10	11.03	0.0027	2.088	0.473	192.0	0.000	94.4	13.31	0.59
07	11.00	0.0034	1.327	1.269	148.7	0.000	96.4	13.55	0.22
08	11.11	0.0054	1.658	0.774	94.2	0.000	95.6	13.57	0.35
12	11.21	-0.0023	1.676	0.546	-	0.000	95.6	13.69	0.52
11	11.24	0.0160	1.613	0.925	31.9	0.000	95.8	13.76	0.30
13	11.39	-0.0048	2.018	0.292	-	0.001	94.8	13.8	1.0
03	11.21	0.0116	1.259	0.885	43.9	0.000	96.7	13.85	0.30
05	10.97	0.0015	0.4010	0.811	341.7	0.000	98.9	13.87	0.33
02	11.26	0.0000	1.287	0.528	20740.0	0.001	96.6	13.91	0.51
04	11.34	0.0039	1.502	0.592	131.6	0.000	96.1	13.93	0.46
06	11.55	0.0013	2.038	1.109	402.1	0.000	94.8	13.99	0.24
01	10.98	0.0074	-0.0491	1.430	68.7	0.000	100.1	14.06	0.19
14	12.30	0.0153	4.178	0.413	33.2	0.000	90.0	14.15	0.71
09	11.11	0.0184	0.0916	0.666	27.8	0.000	99.8	14.17	0.41
Mean age ± 2σ	n=14	MSWD=0.45			1854.7 ±11014.7			13.85	0.18
1279.00-01, Sanidine, J=0.0007135±0.04%, D=1.002±0.001, NM-203D, Lab#=56792									
01	11.24	0.0616	3.154	0.939	8.3	0.000	91.8	13.23	0.33
05	10.98	0.0462	2.172	0.638	11.1	0.001	94.2	13.27	0.45
06	10.88	0.0765	1.292	1.215	6.7	0.000	96.5	13.47	0.24
02	10.84	0.0664	1.148	1.968	7.7	0.000	96.9	13.48	0.16
03	11.00	0.0581	1.650	1.767	8.8	0.000	95.6	13.49	0.17
10	10.94	0.0698	1.362	1.069	7.3	0.000	96.4	13.52	0.26
15	11.05	0.0888	1.716	0.642	5.7	0.000	95.5	13.53	0.43
04	11.03	0.0609	1.523	2.473	8.4	0.000	96.0	13.57	0.12
08	11.02	0.0671	1.238	0.708	7.6	0.000	96.7	13.67	0.39
12	11.26	0.0554	1.911	1.015	9.2	0.000	95.0	13.72	0.27
07	11.74	0.0633	3.410	0.864	8.1	0.000	91.5	13.77	0.32
13	11.09	0.0633	1.095	0.697	8.1	0.000	97.1	13.82	0.39
09	11.32	0.0718	1.455	0.744	7.1	0.000	96.3	13.97	0.37
14	10.99	0.0599	0.1576	0.641	8.5	-0.001	99.6	14.04	0.42
x 11	10.80	0.0279	-0.5624	0.621	18.3	0.000	101.6	14.06	0.44
Mean age ± 2σ	n=11	MSWD=0.45			8.8 ±6.5			13.63	0.15

Notes:
Isotopic ratios corrected for blank, radioactive decay, and mass discrimination, not corrected for interfering reactions.
Errors quoted for individual analyses include analytical error only, without interfering reaction or J uncertainties.
Mean age is weighted mean age of Taylor (1982). Mean age error is weighted error
  of the mean (Taylor, 1982), multiplied by the root of the MSWD where MSWD>1, and also
  incorporates uncertainty in J factors and irradiation correction uncertainties.
Decay constants and isotopic abundances after Steiger and Jäger (1977).
x   symbol preceding sample ID denotes analyses excluded from mean age calculations.
Ages calculated relative to FC-2 Fish Canyon Tuff sanidine interlaboratory standard at 28.02 Ma
Decay Constant (LambdaK (total)) = 5.543e-10/a
Correction factors:
  $(^{39}Ar/^{37}Ar)_{Ca}$ = 0.00068 ± 2e-05
  $(^{36}Ar/^{37}Ar)_{Ca}$ = 0.00028 ± 1e-05
  $(^{38}Ar/^{39}Ar)_K$ = 0.013
  $(^{40}Ar/^{39}Ar)_K$ = 0 ± 0.0004

Appendix B

Table 1. Electron Microprobe data for basaltic tephra.

Sample Point	SiO2	TiO2	Al2O3	FeO	MnO	MgO	CaO	Na2O	K2O	P2O5	SO2	F	Cl	Total
25.37-25.39 mbsf														
06	39.53	0.28	1.05	21.06	0.34	36.50	0.87	0.24	0.13	0.09	0.03	0.00	0.00	100.10
10	39.96	0.03	0.05	18.00	0.25	41.36	0.27	0.02	0.01	0.02	0.01	0.00	0.00	99.98
05	44.18	3.85	13.79	13.14	0.25	9.02	8.25	3.96	1.95	1.18	0.10	0.23	0.08	99.97
11	44.37	4.45	15.66	11.32	0.21	4.87	11.07	3.72	1.70	0.90	0.14	0.22	0.08	98.71
15	45.22	4.24	16.02	11.26	0.22	4.28	9.23	4.56	2.21	1.39	0.15	0.17	0.11	99.05
09	45.36	3.85	17.30	10.38	0.23	4.24	9.40	4.35	1.97	1.27	0.11	0.23	0.11	98.81
13	45.47	3.89	16.56	10.81	0.24	4.58	9.10	4.54	2.18	1.36	0.15	0.20	0.11	99.18
08	45.66	3.77	17.44	10.53	0.25	4.59	8.70	4.55	2.16	1.34	0.11	0.16	0.10	99.35
03	45.68	3.56	17.17	10.60	0.20	4.56	8.53	4.55	2.07	1.38	0.20	0.30	0.08	98.86
12	46.00	3.51	17.00	10.83	0.19	4.51	8.54	4.62	2.09	1.48	0.13	0.25	0.14	99.29
02	46.17	3.56	17.21	10.67	0.24	4.64	8.61	4.75	2.08	1.31	0.13	0.16	0.10	99.63
14	46.47	3.46	17.39	10.62	0.19	4.27	8.25	4.88	2.14	1.44	0.10	0.20	0.11	99.51
01	47.04	3.00	19.67	8.77	0.13	3.69	9.33	4.46	1.75	1.11	0.11	0.13	0.08	99.27
04	48.61	3.02	16.88	10.04	0.19	3.76	7.16	5.12	2.84	1.56	0.08	0.09	0.12	99.47
average	44.98	3.18	14.51	12.00	0.22	9.63	7.67	3.88	1.80	1.13	0.11	0.17	0.09	99.37
25.56-25.57-01 mbsf														
04	39.53	0.13	0.03	20.60	0.37	39.25	0.29	0.00	0.00	0.08	0.00	0.07	0.01	100.35
10	44.57	4.17	15.72	11.25	0.17	4.27	9.17	4.48	2.34	1.41	0.16	0.33	0.10	98.13
06	45.08	4.11	16.35	11.24	0.17	4.58	9.28	4.58	2.13	1.45	0.17	0.22	0.10	99.46
03	45.20	4.31	15.88	11.31	0.20	4.43	9.23	4.63	2.26	1.61	0.12	0.17	0.09	99.44
07	45.74	3.58	16.98	10.47	0.19	4.55	8.81	4.67	2.13	1.33	0.14	0.28	0.19	99.05
05	46.05	3.35	17.30	10.71	0.26	4.18	8.19	4.88	2.15	1.35	0.09	0.16	0.11	98.76
08	46.35	3.60	15.67	10.44	0.17	4.96	10.60	4.04	1.94	0.92	0.10	0.25	0.09	99.14
09	46.63	3.29	17.19	10.41	0.25	4.31	8.16	4.92	2.27	1.41	0.13	0.30	0.11	99.39
01	46.82	3.23	17.34	10.37	0.20	4.24	8.13	4.78	2.28	1.39	0.07	0.14	0.11	99.08
02	51.08	2.30	18.15	9.12	0.23	3.04	5.96	5.67	2.95	1.29	0.03	0.52	0.13	100.46
average	45.71	3.21	15.06	11.59	0.22	7.78	7.78	4.27	2.04	1.22	0.10	0.24	0.10	99.33
25.56-25.57-02 mbsf														
03	39.24	0.20	0.81	20.13	0.41	37.99	0.64	0.23	0.12	0.13	0.02	0.05	0.01	99.98
10	39.32	0.09	0.06	20.62	0.36	38.90	0.26	0.22	0.04	0.09	0.00	0.02	0.13	100.08
18	42.38	2.37	9.08	16.19	0.35	20.46	5.16	2.51	1.26	0.82	0.11	0.15	0.10	100.95
07	44.70	4.33	15.66	11.39	0.20	4.27	9.56	4.62	2.29	1.50	0.17	0.20	0.15	99.04
12	44.85	4.39	15.76	11.35	0.23	4.25	9.70	4.48	2.31	1.47	0.15	0.28	0.10	99.31
01	44.93	4.18	16.13	10.71	0.21	4.55	9.38	4.57	2.09	1.39	0.14	0.15	0.16	98.56
08	44.94	4.55	15.73	10.96	0.24	4.52	9.53	4.57	2.26	1.45	0.15	0.25	0.18	99.31
06	45.01	4.17	15.86	11.08	0.20	4.34	9.12	4.89	2.36	1.45	0.20	0.26	0.23	99.15
16	45.01	4.50	15.77	11.28	0.22	4.26	9.61	4.68	2.34	1.46	0.17	0.25	0.24	99.78
17	45.11	4.29	16.01	11.34	0.22	4.33	9.29	4.55	2.29	1.37	0.18	0.29	0.11	99.38
11	45.44	3.66	16.77	10.91	0.20	4.58	8.72	4.58	2.14	1.45	0.14	0.63	0.12	99.33
04	45.45	3.57	17.05	10.74	0.26	4.52	8.72	4.79	2.18	1.45	0.13	0.31	0.26	99.44
09	45.54	3.69	16.68	11.04	0.23	4.78	8.61	4.68	2.22	1.45	0.16	0.24	0.11	99.42
15	45.77	3.40	17.19	10.64	0.24	4.38	8.37	4.78	2.16	1.47	0.11	0.22	0.21	98.94
13	45.94	3.87	16.72	10.85	0.19	4.36	8.91	4.65	2.29	1.46	0.14	0.24	0.12	99.74
05	45.95	3.69	15.58	11.48	0.22	5.18	11.32	3.68	1.67	0.82	0.19	0.27	0.09	100.13
02	46.08	3.47	17.16	10.46	0.18	4.21	8.25	4.82	2.21	1.44	0.14	0.40	0.08	98.87
14	46.89	3.17	17.37	10.67	0.23	4.01	8.08	4.86	2.27	1.47	0.12	0.16	0.19	99.47
average	44.58	3.42	14.19	12.32	0.24	9.10	7.96	4.01	1.92	1.23	0.13	0.24	0.14	99.49

Table 1. continued

Sample Point	SiO2	TiO2	Al2O3	FeO	MnO	MgO	CaO	Na2O	K2O	P2O5	SO2	F	Cl	Total
92.46-92.50 mbsf														
02	41.40	3.32	12.70	12.27	0.24	13.32	8.32	3.44	1.74	0.86	0.06	0.04	0.11	97.82
07	42.38	4.30	15.69	10.20	0.24	4.49	10.94	4.62	2.37	1.22	0.10	0.17	0.11	96.83
06	42.40	4.27	15.81	10.13	0.16	4.26	10.68	4.50	2.34	1.24	0.11	0.03	0.10	96.03
04	42.59	4.22	15.96	10.20	0.18	4.72	10.92	6.79	2.30	1.11	0.23	0.16	0.14	99.52
03	42.61	4.46	15.51	10.27	0.15	4.56	10.70	4.63	2.30	1.35	0.09	0.25	0.11	96.98
08	42.63	4.27	15.58	10.09	0.29	4.47	10.91	4.65	2.44	1.21	0.12	0.31	0.10	97.07
01	42.75	4.18	15.74	10.23	0.22	4.53	10.99	4.47	2.49	1.37	0.12	0.45	0.13	97.64
05	43.20	4.22	16.04	10.19	0.24	4.40	10.91	4.79	2.43	1.20	0.13	0.34	0.13	98.20
48	43.38	4.25	15.97	10.09	0.21	4.19	10.54	4.64	2.51	1.20	0.10	0.37	0.12	97.56
average	42.59	4.16	15.44	10.41	0.21	5.44	10.54	4.73	2.32	1.20	0.12	0.23	0.12	97.52
112.51-112.52 mbsf														
05	40.95	4.61	15.14	11.89	0.22	5.46	13.39	3.55	1.69	0.88	0.12	0.35	0.09	98.34
01	41.52	4.87	13.68	9.85	0.12	7.58	16.45	2.67	1.17	0.62	0.12	0.14	0.06	98.82
02	41.99	4.37	15.56	11.76	0.23	4.98	11.85	4.01	1.81	1.02	0.11	0.08	0.10	97.88
04	42.13	4.61	15.95	12.00	0.20	4.82	11.41	4.27	2.02	1.09	0.15	0.25	0.09	99.00
03	42.69	4.25	13.62	10.48	0.15	6.99	15.18	2.92	1.28	0.75	0.10	0.14	0.07	98.63
average	41.86	4.54	14.79	11.20	0.19	5.97	13.66	3.48	1.59	0.87	0.12	0.19	0.08	98.53
136.21-136.27 mbsf														
04	44.66	3.77	15.84	11.16	0.25	4.56	9.28	4.91	2.27	0.06	1.14	0.22	0.15	98.27
02	44.69	3.76	16.00	11.20	0.23	4.18	9.46	4.91	2.20	0.09	1.31	0.07	0.11	98.21
01	44.83	3.55	16.06	11.24	0.26	4.02	9.25	4.81	2.28	0.09	1.41	0.13	0.12	98.06
03	44.98	3.79	16.19	11.02	0.18	4.19	9.17	4.89	2.32	0.05	1.13	0.15	0.13	98.19
average	44.79	3.72	16.02	11.16	0.23	4.24	9.29	4.88	2.27	0.07	1.25	0.14	0.13	98.18
140.30-140.36 mbsf														
19	44.77	3.75	15.85	10.74	0.22	4.18	9.60	5.02	2.27	1.30	0.12	0.44	0.12	98.38
01	44.81	3.97	15.92	10.91	0.23	4.27	9.48	4.72	2.28	1.21	0.08	0.52	0.14	98.56
12	44.87	3.79	16.33	10.57	0.24	4.11	9.38	4.91	2.28	1.22	0.08	0.25	0.13	98.16
14	44.91	3.71	16.06	10.97	0.18	4.29	9.33	4.96	2.34	1.24	0.09	0.35	0.13	98.54
20	44.95	3.84	16.26	10.60	0.18	4.26	9.65	4.72	2.20	1.19	0.09	0.23	0.11	98.27
15	45.01	3.81	16.29	10.64	0.23	4.22	9.44	4.99	2.22	1.21	0.12	0.69	0.14	99.02
16	45.02	3.75	16.19	10.77	0.18	4.19	9.55	4.82	2.22	1.24	0.11	0.47	0.16	98.67
06	45.03	3.69	16.14	10.87	0.22	4.40	9.57	5.06	2.26	1.29	0.07	0.15	0.12	98.88
11	45.04	3.62	16.18	10.66	0.24	4.14	9.21	4.84	2.21	1.32	0.11	0.32	0.13	98.02
05	45.06	3.79	16.54	10.81	0.20	4.31	9.48	4.78	2.29	1.17	0.06	0.12	0.13	98.72
25	45.11	3.66	16.00	10.91	0.22	4.32	9.10	4.73	2.25	1.13	0.18	0.59	0.16	98.36
09	45.14	3.72	16.51	10.50	0.24	4.24	9.71	4.81	2.17	1.26	0.14	0.38	0.10	98.91
08	45.20	3.96	16.20	10.69	0.23	4.18	9.39	4.97	2.22	1.24	0.07	0.19	0.13	98.67
03	45.22	3.76	16.31	10.81	0.20	4.33	9.58	4.92	2.19	1.16	0.06	0.18	0.14	98.88
04	45.25	3.54	16.46	10.40	0.27	4.28	9.37	4.72	2.20	1.24	0.08	0.41	0.12	98.34
02	45.31	3.80	16.19	10.79	0.23	4.21	9.36	4.84	2.28	1.24	0.08	0.39	0.14	98.85
22	45.34	3.53	16.27	10.77	0.30	4.07	9.29	5.01	2.38	1.44	0.11	0.21	0.14	98.87
17	45.36	3.78	16.31	10.65	0.28	4.39	9.46	4.92	2.20	1.28	0.08	1.11	0.13	99.93
21	45.41	3.84	16.36	10.95	0.23	4.16	9.67	5.00	2.32	1.31	0.08	0.38	0.12	99.83
13	45.45	3.68	16.26	10.63	0.18	4.20	9.51	4.69	2.19	1.23	0.10	0.70	0.14	98.96
23	45.48	3.55	16.10	10.79	0.27	4.31	9.41	4.99	2.30	1.26	0.06	0.83	0.12	99.46
24	45.50	3.72	16.45	10.86	0.20	4.32	9.23	4.98	2.25	1.23	0.13	0.14	0.13	99.15
10	45.51	3.64	16.31	10.75	0.26	4.05	9.03	5.02	2.36	1.36	0.12	0.53	0.10	99.04
07	45.64	3.77	16.24	10.84	0.23	4.00	9.29	5.01	2.48	1.39	0.11	0.24	0.12	99.36
18	45.81	3.57	16.44	10.66	0.26	4.14	9.21	5.04	2.33	1.57	0.07	0.18	0.11	99.40
average	45.21	3.73	16.25	10.74	0.23	4.22	9.41	4.90	2.27	1.27	0.10	0.40	0.13	98.85

Table 1. continued

Sample Point	SiO2	TiO2	Al2O3	FeO	MnO	MgO	CaO	Na2O	K2O	P2O5	SO2	F	Cl	Total
145.12-145.16 mbsf														
16	0.04	0.03	0.00	0.03	-0.01	-0.04	0.03	0.01	0.00	0.02	0.25			0.41
18	8.23	0.31	0.96	0.91	0.03	0.25	0.59	0.27	0.14	0.16	0.65	-0.15	1.36	13.87
20	8.59	0.37	0.92	0.67	0.01	0.21	0.50	0.28	0.15	0.06	0.35	-1.61	1.36	13.47
06	10.35	0.55	2.33	1.55	0.03	0.60	1.33	0.76	0.34	0.22	0.31	-0.48	1.30	19.67
11	15.16	0.40	1.06	0.92	0.03	0.13	0.38	0.19	0.09	0.09	0.99	-0.46	1.45	20.90
21	20.24	1.40	6.84	3.73	0.07	1.64	3.65	1.78	0.93	0.53	0.29	-7.79	0.98	42.07
03	22.08	1.24	4.28	2.94	0.08	1.07	2.57	1.19	0.62	0.38	0.32	-0.33	1.02	37.77
07	27.17	1.53	5.98	3.80	0.08	1.43	3.63	1.83	0.91	0.60	0.28	0.06	0.78	48.09
15	27.58	10.04	11.71	29.74	0.34	4.57	5.30	3.64	1.34	0.81	0.04	-0.65	0.10	95.22
04	44.66	3.24	14.02	9.11	0.13	3.69	8.33	4.54	1.96	1.19	0.13	-4.67	0.22	91.23
05	44.68	3.16	11.42	8.09	0.15	4.60	9.91	0.33	1.60	1.04	0.10	-0.28	0.27	85.34
02	44.73	3.62	15.71	10.13	0.24	4.17	9.17	4.99	2.39	1.32	0.11	-5.77	0.11	96.69
14	44.74	3.61	15.37	10.38	0.23	3.92	9.31	5.27	2.44	1.55	0.09	0.13	0.12	97.15
01	45.66	3.62	15.67	10.18	0.28	4.17	9.10	4.82	2.41	1.31	0.06	-6.23	0.16	97.43
13	46.22	3.03	6.03	7.69	0.19	12.33	21.80	0.59	0.10	0.09	0.03	0.12	0.01	98.23
19	46.92	3.58	16.68	10.52	0.22	4.07	9.42	3.58	1.97	1.50	0.08			98.55
08	47.03	2.23	20.10	6.00	0.08	2.20	10.04	4.35	1.50	0.91	0.07	-6.13	0.10	94.62
09	49.21	1.45	23.12	3.44	0.05	1.29	10.78	3.90	0.89	0.58	0.03	0.19	0.09	95.03
12	49.90	0.75	27.16	2.28	0.06	0.70	12.45	4.09	0.66	0.32	0.07	-0.44	0.02	98.46
10	52.20	0.92	14.95	1.03	0.01	0.31	6.56	2.11	0.32	0.28	0.15	0.05	0.35	79.24
17	52.55	3.81	10.70	7.63	0.17	2.64	6.10	3.29	1.54	1.81	1.21	-0.19	0.18	91.63
average	33.71	2.33	10.72	6.23	0.12	2.57	6.71	2.47	1.06	0.70	0.27	-1.82	0.53	67.38

Table 2. Electron Microprobe data for feldspar phenocrysts.

Sample Point	SiO2	Al2O3	FeO	CaO	Na2O	K2O	SrO	BaO	H2O	Total
481.80-481.82 mbsf										
2	65.81	20.43	0.22	0.99	7.54	5.07	0.03	0.11	0.00	100.20
3	65.64	20.73	0.26	1.15	7.45	5.15	0.10	0.29	0.00	100.77
4	40.84	32.82	0.31	0.16	23.87	1.24	0.00	0.06	0.00	99.31
5	65.44	20.72	0.20	1.44	7.60	4.86	0.06	0.12	0.00	100.42
6	63.82	18.34	0.11	0.02	0.84	15.54	0.01	0.05	0.00	98.73
7	66.35	19.67	0.13	0.28	6.22	7.63	0.03	0.00	0.00	100.31
8	65.81	20.02	0.13	0.88	7.02	6.09	0.00	0.06	0.00	100.01
average	61.96	21.82	0.19	0.70	8.65	6.51	0.03	0.10	0.00	99.96